

E. WOLF, PROGRESS IN OPTICS VVV
© 199X
ALL RIGHTS RESERVED

X

**Optical Solitons in Periodic Media with Resonant and Off-Resonant
Nonlinearities**

BY

GERSHON KURIZKI*

ALEXANDER E. KOZHEKIN†

TOMÁŠ OPATRNÝ‡
*Department of Chemical Physics,
Weizmann Institute of Science,
Rehovot 76100, ISRAEL*

BORIS MALOMED
*Department of Interdisciplinary Studies,
Faculty of Engineering,
Tel Aviv University, Tel Aviv 69978, Israel*

*E-mail: Gershon.Kurizki@weizmann.ac.il

†Present address: *Institute of Physics and Astronomy, University of Aarhus, Ny Munkegade,
DK-8000 Aarhus C, Denmark*

‡Present address: *Friedrich-Schiller-Universität Jena, Theoretisch-Physikalisches Institut,
Max-Wien Platz 1, 07743 Jena, Germany and Palacký University, Faculty of Natural Sciences,
Svobody 26, 77146 Olomouc, Czech Republic*

CONTENTS¹

	PAGE
§ 1. INTRODUCTION	3
§ 2. SOLITONS IN BRAGG GRATINGS WITH CUBIC AND QUADRATIC NONLINEARITIES	6
§ 3. SELF-INDUCED TRANSPARENCY (SIT) IN UNIFORM MEDIA AND THIN FILMS	11
§ 4. SIT IN RESONANTLY ABSORBING BRAGG REFLECTORS (RABR): THE MODEL	15
§ 5. BRIGHT SOLITONS IN RABR	24
§ 6. DARK SOLITONS IN RABR	33
§ 7. LIGHT BULLETS (SPATIOTEMPORAL SOLITONS)	38
§ 8. EXPERIMENTAL PROSPECTS AND CONCLUSIONS	41
REFERENCES	43

¹Run LaTeX twice for up-to-date contents.

§1. Introduction

The study of light-matter interactions in dielectric structures with periodic modulation of the refractive index has developed into a vast research area. At the heart of this area is the interplay between Bragg reflections, which block the propagation of light in spectral bands known as photonic band gaps (PBGs), and the dynamical modifications of these reflections by *nonlinear* light-matter interactions (see bibliography compiled by Dowling and Everitt [2000]). Three- or two-dimensional (3D or 2D) PBGs are needed in order to extinguish spontaneous emission in all possible directions of propagation, which requires the nontrivial fabrication of 3D- or 2D-periodic photonic crystals (Yablonovitch [1987], Yablonovitch [1993]). For controlling strictly unidirectional propagation, it is sufficient to resort to PBGs in one-dimensional (1D) periodic structures (Bragg reflectors or dielectric multi-layer mirrors). Illumination of the periodic dielectric structure at a PBG frequency in the limit of vanishing nonlinearity leads to exponential decay of the incident field amplitude with penetration depth, at the expense of exponential growth of the back-scattered (Bragg-reflected) amplitude. However, this reflection may weaken or cease altogether, rendering the structure transparent, when the illumination intensity and the resulting nonlinearity modify the refractive index so as to shift (or even close down) the PBG. The pulsed mode of propagation in nonlinear periodic structures exhibits a variety of fundamentally unique and technologically interesting regimes: nonlinear filtering, switching, and distributed-feedback amplification (Scalora, Dowling, Bowden and Bloemer [1994a], Scalora, Dowling, Bowden and Bloemer [1994b]). Among these regimes, we have chosen here to concentrate on the intriguing solitary waves existing in PBGs, known as *gap solitons* (GS), and solitons propagating near PBGs.

A GS is usually understood as a self-localized moving or standing (quiescent) bright region, where light is confined by Bragg reflections against a dark background. The soliton spectrum is tuned away from the Bragg resonance by the nonlinearity at sufficiently high field intensities. There is also considerable physical interest in finding in the vicinity of a PBG a dark soliton (DS), i.e., a ‘hole’ of a fixed shape in a continuous-wave (cw) background field of constant intensity (Kivshar and Luther-Davies [1998]).

The first type of GS was predicted to exist in a Bragg grating filled with a Kerr medium, whose nonlinearity is cubic (Christodoulides and Joseph [1989], Aceves and Wabnitz [1989], Feng and Kneubuhl [1993]). Detailed theoretical studies of these *Bragg-grating (Kerr-nonlinear) solitons* (see de Sterke and Sipe [1994] for a review) were followed by their experimental observation (Eggleton, Slusher, de Sterke, Krug and Sipe [1996]) in a short (< 10 cm) piece of an optical fiber with a resonant Bragg grating written on it. In theoretical considerations of solitons in a Bragg grating combined with Kerr nonlinearity, a formidable problem is their stability. Current experiments are conducted in short fiber pieces, which do not allow us to test the solitons’ stability. Approximate and rigorous treatments of the stability problem (Malomed and Tasgal [1994], Barashenkov, Pelinovsky and Zemlyanaya [1998], de Rossi, Conti and Trillo [1998]) have demonstrated that the Kerr-nonlinear Bragg-grating solitons have instability regions in their frequency-amplitude parametric plane, far from the PBG-center, small-amplitude limit. The generation of a slow gap soliton in a Kerr - nonlinear periodic grating via Raman transfer of en-

ergy from the pump pulse to the Bragg - resonant Stokes components was recently proposed by Winful and Perlin [2000].

A Bragg grating with quadratic or second-harmonic-generating (SHG) nonlinearity can also give rise to a rich spectrum of solitons (Peschel, Peschel, Lederer and Malomed [1997], He and Drummond [1997], Conti, Trillo and Assanto [1997]). This model has been shown to possess a number of remarkable features. In particular (Peschel, Peschel, Lederer and Malomed [1997]), contrary to Kerr-nonlinear Bragg gratings, in the case of SHG nonlinearity the gap in which solitons may exist is partly *empty*, only part of it being filled with actually existing soliton solutions.

While the above temporal-domain models pertain to light propagation in fibers, distributions of stationary fields in a planar (2D) nonlinear optical waveguide are governed by spatial-domain equations (Stegeman and Segev [1999]). In the planar waveguide, a Bragg grating can be realized as a system of parallel ‘scratches’. The soliton spectrum of this model contains (Mak, Malomed and Chu [1998b]) not only the fundamental single-humped solitons but also their two-humped bound states, which, quite unusually, turn out to be dynamically stable. Moreover, it possesses (Champneys and Malomed [2000]), besides the conventional GSs, also *embedded solitons*, which are isolated solitary-wave solutions within the continuous spectrum, rather than inside the gap.

A principally different mechanism of GS formation has been discovered in a periodic array of thin layers of *resonant two-level systems* (TLS) separated by half-wavelength nonabsorbing dielectric layers, i.e., a *resonantly absorbing Bragg reflector* (RABR) (Kozhekin and Kurizki [1995], Kozhekin, Kurizki and Malomed [1998], Opatrný, Malomed and Kurizki [1999]). The RABR has been found to allow, for *any* Bragg reflectivity, a vast family of stable solitons, both standing and moving (Kozhekin and Kurizki [1995], Kozhekin, Kurizki and Malomed [1998]). As opposed to the 2π -solitons arising in self-induced transparency, i.e., resonant field – TLS interaction in uniform media (McCall and Hahn [1969], McCall and Hahn [1970]), gap solitons in RABR may have an *arbitrary* pulse area (Kozhekin and Kurizki [1995], Kozhekin, Kurizki and Malomed [1998]). As shown below, GS solutions have been consistently obtained only in a RABR with *thin* active TLS layers. By contrast, an attempt (Aközbeke and John [1998]) to obtain such solutions in a periodic structure *uniformly* filled with active TLS is physically unfounded, and fails for many parameter values, so that such generalization remains an open problem (see Sec. 4.3 below).

An unexpected property of the RABR is that, alongside the stable bright-soliton solutions (Kozhekin and Kurizki [1995], Kozhekin, Kurizki and Malomed [1998]), this system gives rise to a family of dark solitons (DSs), a large part of which are *stable* (Opatrný, Malomed and Kurizki [1999]). While the existence of stable bright-soliton solutions along with *unstable* DSs is a known feature of uniform SHG media (Kivshar and Luther-Davies [1998]), a RABR with thin active layers provides, to the best of our knowledge, the first example of a nonlinear optical medium in which *stable* bright and dark solitons exist for the *same values* of the model’s parameters (albeit at different frequencies). It is also the first example of the existence of stable bright solitons alongside *stable cw* (*background*) solutions.

Potential applications of GSs are based on the system’s ability to filter out (by means of Bragg reflections) all pulses except for those satisfying the GS dispersion condition, as well as to control the pulses’ shape and velocity. It would be clearly

desirable to supplement these advantageous properties by immunity to transverse diffraction of the pulse, i.e., to achieve *simultaneous* transverse and longitudinal self-localization of light in a RABR. This motivates a quest for multi-dimensional solitons that are localized in both space and time.

The concept of optical multi-dimensional spatio-temporal solitons, alias ‘light bullets’ (LBs), was pioneered by Silberberg (Silberberg [1990]), and has since been investigated in various nonlinear optical media, with particular emphasis on the stability of LBs. For a SHG medium, the existence of stable two- and three-dimensional (2D and 3D) solitons was predicted as early as in 1981 (Kanashov and Rubenchik [1981]), followed by detailed studies of their propagation and stability against collapse (Hayata and Koshihara [1993], Malomed, Drummond, He, Berntson, Anderson and Lisak [1997], Mihalache, Mazilu, Malomed and Torner [1998], He and Drummond [1998]), Recently, the first experimental observation of a quasi-2D spatiotemporal soliton in a 3D SHG sample was reported (Liu, Qian and Wise [1999]). The concept of *dark* LBs was proposed by Chen and Atai [1995]). Stable *antidark* LBs, i.e., those supported by a finite cw background, were predicted in a generalized nonlinear Schrödinger equation which contains third-order temporal dispersion (Frantzeskakis, Hizanidis, Malomed and Polymilis [1998]).

As early as in 1984, simulations indicated that self-focusing of spatiotemporal pulses in a SIT medium could result in the formation of a quasi-stable vibrating object (Drummond [1984]), which was a hint at the possible existence of LBs. It has analytically been demonstrated (Blaauboer, Malomed and Kurizki [2000]) that uniform 2D and 3D SIT media can indeed carry stable LBs. This investigation has been extended to the case of RABR, wherein stable, transversely localized SIT solutions combining LB and GS properties are predicted (Blaauboer, Kurizki and Malomed [2000]). RABR with *any* Bragg reflectivity can support stable LBs, which are closely related to those in uniform SIT media (Blaauboer, Malomed and Kurizki [2000]). 2D LBs supported by a combination of a Bragg reflector with SHG nonlinearity were theoretically investigated still earlier (He and Drummond [1998]).

Finally, we briefly mention a topic that is outside the scope of this review, namely, *quantum bright solitons*, which have been a subject of extensive studies in recent years. It has been established that solitons are superpositions of quantum states that correspond to clusters of photons bound together. Most of the initial activity in this area was devoted to Kerr-nonlinear fiber solitons (Lai and Haus [1989a], Lai and Haus [1989b], Wright [1991], Yudson [1985], Kärtner and Haus [1993], Cheng [1991]). It was shown that optical fiber solitons have quantum analogs which are described by the quantum nonlinear Schrödinger equation (QNLSE). The motivation was to gain understanding of squeezing effects in soliton propagation (Carter, Drummond, Reid and Shelby [1987], Watanabe, Nakano, Honold and Yamamoto [1989], Drummond, Carter and Shelby [1989], Haus and Lai [1990], Rosenbluh and Shelby [1991] see a review by Sizmman and Leuchs [1999]), two-photon binding effects (Deutsch, Chiao and Garrison [1992], Deutsch, Chiao and J.C.Garrison [1993]), and fundamental limits imposed on communication systems employing solitons (Drummond, Shelby, Friberg and Yamamoto [1993], Chiao, Deutsch, Garrison and Wright [1993]). Multidimensional quantum solitons were predicted in Kerr and SHG waveguides (Drummond and He [1997], Kheruntsyan and Drummond [1998b], Kheruntsyan and Drummond [1998a], Kheruntsyan and Drummond [2000]).

The quantization of GSs has attracted considerable attention as well. A Bethe-

ansatz solution was given (Cheng and Kurizki [1995]) for quantum GSs consisting of pairwise interacting massive photons (in the effective-mass regime of PBGs propagation) in Kerr-nonlinear 1D periodic grating. A mechanism has been found for the creation of two-photon bound states by photons resonantly interacting with identical two-level atoms near PBGs in 1D periodic structures (Kurizki, Kofman, Kozhokin and Cheng [1996]). A Bethe ansatz solution for photons in a PBG material interacting with a single atom was obtained by Rupasov and Singh [1996a], Rupasov and Singh [1996b]. It has later been generalized to an extended many-atom periodic system, where quantum GSs involving pairs of photons and propagating inside a PBG have been found (John and Rupasov [1999]). This subject is of potential interest for quantum communications via entangled two-photon states.

This review starts with a brief survey of solitons in Bragg gratings with cubic and quadratic nonlinearities (Ch. 2) and of self-induced transparency (SIT) in uniform media and thin films (Ch. 3). It then continues with the derivation of the model for phenomena similar to SIT in resonantly absorbing Bragg reflectors (RABR) (Ch. 4). Bright and dark solitons in RABR are discussed in Ch. 5 and 6, consecutively. Light bullets in periodic resonantly-absorbing media are treated in Ch. 7. Finally, the prospects for experimental progress in this area are summarized in Ch. 8.

§ 2. Solitons in Bragg gratings with cubic and quadratic nonlinearities

2.1. KERR NONLINEARITY

Because the Bragg grating gives rise to very strong effective dispersion, its combination with various optical nonlinearities can create a rich variety of solitons, which, in most cases, are *gap solitons* (GSs), as their intrinsic frequency must belong to a gap in the spectrum of *linear* waves in the Bragg grating. Initially, a Bragg grating filled with a Kerr nonlinear medium, whose nonlinearity is cubic, was considered by Christodoulides and Joseph [1989], Aceves and Wabnitz [1989], and Feng and Kneubuhl [1993]. The corresponding system of two propagation equations for the right (forward)- and left (backward)-traveling field envelopes $\mathcal{E}_F(\zeta, \tau)$ and $\mathcal{E}_B(\zeta, \tau)$ with the self- and cross-phase-modulation cubic terms is a generalization of the known Thirring model (in the Thirring model proper, the self-phase modulation terms are omitted):

$$i \frac{\partial \mathcal{E}_F}{\partial \tau} + i \frac{\partial \mathcal{E}_F}{\partial \zeta} + \left(|\mathcal{E}_B|^2 + \frac{1}{2} |\mathcal{E}_F|^2 \right) \mathcal{E}_F + \mathcal{E}_B = 0, \quad (2.1a)$$

$$i \frac{\partial \mathcal{E}_B}{\partial \tau} - i \frac{\partial \mathcal{E}_B}{\partial \zeta} + \left(|\mathcal{E}_F|^2 + \frac{1}{2} |\mathcal{E}_B|^2 \right) \mathcal{E}_B + \mathcal{E}_F = 0. \quad (2.1b)$$

Here the dimensionless time τ and length ζ are related to the physical time t and length z as $t = 4\tau/(a_1\omega_c)$, and $z = 4c\zeta/(a_1\omega_cn_0)$, where n_0 is the mean linear index of refraction, a_1 is its modulation (see Eq. (4.1) below), and ω_c is the central frequency of the band gap. Actual values of the electric fields can be obtained from the dimensionless quantities $\mathcal{E}_{F,B}$ upon multiplication by $\omega_c \sqrt{a_1 n_0 / (48\pi\chi^{(3)})}$, where $\chi^{(3)}$ is the third order susceptibility. In Ch. 4.1 we present a general derivation of the Maxwell equations in Bragg gratings.

The existence of solitons in a given model is usually closely related to the modulational instability of a continuous-wave (cw) solution in the model (Agrawal [1995]):

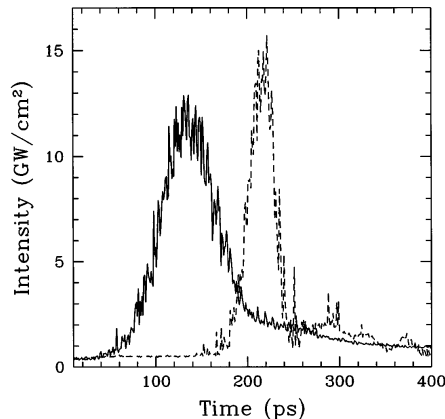


Figure 1: Experimental evidence for the existence of solitons in a nonlinear optical fiber with Bragg grating: the broad pulse is far from a Bragg resonance and has passed the fiber without interacting with the grating; the narrow one is a soliton shaped by Bragg-resonant interaction with the grating (see further details in the work by Eggleton, Slusher, de Sterke, Krug and Sipe [1996]).

an array (chain) of bright solitons can be generated from the cw solution by modulational instability. In an optical fiber combining a Bragg grating and Kerr nonlinearity, *all* the cw states are modulationally unstable, as observed in a direct experiment (which also involved the polarization of light) by Slusher, Spalter, Eggleton, Pereira and Sipe [2000]. However, as was shown by Opatrný, Malomed and Kurizki [1999] (see Ch. 6 below) a RABR gives rise to stable bright solitons coexisting with *stable* cw states, which is a very unusual property.

Unlike the Thirring model proper, its optical version based on Eqs. (2.1a) and (2.1b) is not integrable. Moreover, the equations lack any invariance with respect to the reference frame (i.e., the model is neither Galilean nor Lorentz invariant). Nevertheless, *exact* single-soliton solutions, which contain two independent parameters, viz., an intrinsic frequency ω and the soliton's velocity v , were found in the above-mentioned works by Christodoulides and Joseph [1989] and Aceves and Wabnitz [1989], following the pattern of the Thirring-model solitons. At $v = 0$, the quiescent (standing) solitons *completely* fill the gap $-1 < \omega < +1$ in the spectrum of the linearized equations (2.1a) and (2.1b), and the velocity takes all the possible values $-1 < v < +1$ (recall that, in the present notation, the maximum group velocity of light is 1). Solitons with small frequencies have small amplitudes and are close to the classical nonlinear Schrödinger (NLS) solitons, while the ones with values of ω^2 closer to 1 are strongly different from their NLS counterparts; in particular, they are *chirped*, i.e., they have a nontrivial intrinsic phase structure.

Many properties of these *Bragg-grating solitons*, as they are frequently called, were reviewed by de Sterke and Sipe [1994] (see also the special issue of *Optics Express* edited by Brown and Eggleton [1998]). Detailed theoretical studies were finally followed by their experimental observation by Eggleton, Slusher, de Sterke,

Krug and Sipe [1996] in a short (< 10 cm) piece of an optical fiber with a resonant Bragg grating written on it. This experiment requires the use of very powerful light beams, with an intensity comparable to the fiber's breakdown threshold. Despite this difficulty, propagating pulses with soliton-like shapes have been detected in the experiment, see Fig. 1.

It should be stressed that the above-mentioned exact soliton solutions to Eqs. (2.1a) and (2.1b) take the simplest form in the case $v = 0$, corresponding to a pulse of *standing light*. In reality, the soliton observed by Eggleton, Slusher, de Sterke, Krug and Sipe [1996] was moving at a considerable velocity. Generation and detection of *zero-velocity* solitons in nonlinear Bragg gratings remains an experimental challenge.

Theoretical considerations of solitons in Bragg gratings with Kerr nonlinearity face the tough problem of soliton stability. The first approach to the stability problem, developed by Malomed and Tasgal [1994] was based on the variational approximation. Although this approach is not rigorous, it clearly demonstrates that, sufficiently far from the above-mentioned NLS (small-frequency small-amplitude) limit, Bragg-grating solitons can be *unstable*. Later, a rigorous analysis of the same stability problem was developed by Barashenkov, Pelinovsky and Zemlyanaya [1998] and by de Rossi, Conti and Trillo [1998]. It has been demonstrated that the Bragg-grating solitons indeed have instability regions in their parametric (ω, v) plane, which are close to those originally predicted by means of the variational approximation.

The derivation of the standard equations (2.1a) and (2.1b) from the underlying Maxwell's equations (see Ch.. 4.1) neglects all the linear terms with second-order derivatives (which account for the material dispersion and/or diffraction in the medium). As shown by Champneys, Malomed and Friedman [1998], taking the second derivatives into account drastically changes the soliton *content of the model* (although the propagation distance necessary to observe the change of the solitons' shape may be much larger than that available in current experiments). The relatively simple soliton solutions generated by Eqs. (2.1a) and (2.1b) immediately disappear after the inclusion of the second-derivative terms; instead, three completely new branches of soliton solutions emerge, provided that the coefficient in front of the second-derivative terms exceeds a certain minimum value. Very recently, it has been shown by Schöllmann and Mayer [2000] that these new branches are, generally, also subject to an instability.

Finally, we mention a *dual-core* nonlinear optical fiber, each core containing a Bragg grating, which is described by four equations (Mak, Malomed and Chu

[1998a]),

$$\begin{aligned} i\frac{\partial\mathcal{E}_{F1}}{\partial\tau} + i\frac{\partial\mathcal{E}_{F1}}{\partial\zeta} + \left(\frac{1}{2}|\mathcal{E}_{F1}|^2 + |\mathcal{E}_{B1}|^2\right)\mathcal{E}_{F1} \\ + \mathcal{E}_{B1} + \lambda\mathcal{E}_{F2} = 0, \end{aligned} \quad (2.2a)$$

$$\begin{aligned} i\frac{\partial\mathcal{E}_{B1}}{\partial\tau} - i\frac{\partial\mathcal{E}_{B1}}{\partial\zeta} + \left(\frac{1}{2}|\mathcal{E}_{B1}|^2 + |\mathcal{E}_{F1}|^2\right)\mathcal{E}_{B1} \\ + \mathcal{E}_{F1} + \lambda\mathcal{E}_{B2} = 0, \end{aligned} \quad (2.2b)$$

$$\begin{aligned} i\frac{\partial\mathcal{E}_{F2}}{\partial\tau} + i\frac{\partial\mathcal{E}_{F2}}{\partial\zeta} + \left(\frac{1}{2}|\mathcal{E}_{F2}|^2 + |\mathcal{E}_{B2}|^2\right)\mathcal{E}_{F2} \\ + \mathcal{E}_{B2} + \lambda\mathcal{E}_{F1} = 0, \end{aligned} \quad (2.2c)$$

$$\begin{aligned} i\frac{\partial\mathcal{E}_{B2}}{\partial\tau} - i\frac{\partial\mathcal{E}_{B2}}{\partial\zeta} + \left(\frac{1}{2}|\mathcal{E}_{B2}|^2 + |\mathcal{E}_{F2}|^2\right)\mathcal{E}_{B2} \\ + \mathcal{E}_{F2} + \lambda\mathcal{E}_{B1} = 0, \end{aligned} \quad (2.2d)$$

where the subscripts 1 and 2 stand for the core number, the dimensionless quantities τ , ζ , $\mathcal{E}_{B,F;1,2}$ have the same meaning as in Eq. (2.1), and λ is the real linear coupling between the cores. Due to this linear coupling, a soliton in this system necessarily has its components in both cores. As shown by Mak, Malomed and Chu [1998a], an obviously symmetric soliton with equal components in the two cores, $\mathcal{E}_{F1} = \mathcal{E}_{F2}$ and $\mathcal{E}_{B1} = \mathcal{E}_{B2}$, becomes unstable when its energy exceeds a certain threshold. The instability gives rise to a *pitchfork bifurcation* that generates a pair of stable asymmetric solitons which are mirror images of each other.

2.2. QUADRATIC NONLINEARITIES

A Bragg grating with quadratic (second-harmonic-generating, SHG) nonlinearity gives rise to a vast variety of solitons. This model was introduced independently and simultaneously by Peschel, Peschel, Lederer and Malomed [1997], He and Drummond [1997], and Conti, Trillo and Assanto [1997]. The model includes four fields, namely, the fundamental- and second-harmonic components of the forward- (F-) and backward- (B-) traveling waves. In a normalized notation, the corresponding system takes the form

$$i\frac{\partial\mathcal{E}_F}{\partial\tau} + i\frac{\partial\mathcal{E}_F}{\partial\zeta} + \chi\mathcal{E}_F + \mathcal{E}_F^*\mathcal{G}_F + \mathcal{E}_B = 0, \quad (2.3a)$$

$$i\frac{1}{v}\frac{\partial\mathcal{G}_F}{\partial\tau} + i\frac{\partial\mathcal{G}_F}{\partial\zeta} + \chi^{-1}\mathcal{G}_F + \mathcal{E}_F^2 + \varkappa\mathcal{G}_B = 0, \quad (2.3b)$$

$$i\frac{\partial\mathcal{E}_B}{\partial\tau} - i\frac{\partial\mathcal{E}_B}{\partial\zeta} + \chi\mathcal{E}_B + \mathcal{E}_B^*\mathcal{G}_B + \mathcal{E}_F = 0, \quad (2.3c)$$

$$i\frac{1}{v}\frac{\partial\mathcal{G}_B}{\partial\tau} - i\frac{\partial\mathcal{G}_B}{\partial\zeta} + \chi^{-1}\mathcal{G}_B + \mathcal{E}_B^2 + \varkappa\mathcal{G}_F = 0, \quad (2.3d)$$

where \mathcal{E} and \mathcal{G} are the fundamental- and second-harmonic fields, $v > 0$ is the group velocity of the second harmonic relative to the fundamental harmonic, \varkappa is a (generally complex) coupling F-B coefficient in the second harmonic, given that the coupling constant at the fundamental harmonic is normalized to 1, and the real parameter χ determines the *phase mismatch* of the two harmonics.

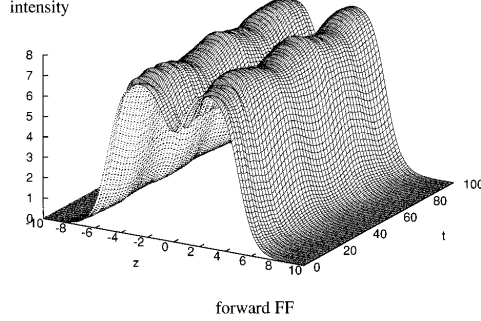


Figure 2: An example of a dynamically stable double-humped soliton in the model based on Eqs. (2.3a) - (2.3d), combining a Bragg grating and second-harmonic-generation nonlinearity. Shown in this figure is the intensity of the forward fundamental-harmonic component $|\mathcal{E}_F|^2$ (see Peschel, Peschel, Lederer and Malomed [1997]).

Analytical and numerical consideration of solitons in this model has revealed a number of nontrivial features. In particular, Peschel, Peschel, Lederer and Malomed [1997] have found that, contrary to the model (2.1) with Kerr nonlinearity, in the system (2.3) the gap in which solitons may exist has *voids*, so that only a part of it is filled with actually existing soliton solutions. Another noteworthy finding of the same work is that not only single-humped fundamental solitons, but also their two-humped bound states, which are normally unstable in other versions of the SHG models, are *dynamically stable* in the four-wave model (2.3). An example of a two-humped soliton which turns out to be fairly stable in simulations of the system (2.3) is shown in Fig. 2. A detailed description of gap solitons in the four-wave model combining a Bragg grating and SHG nonlinearity can be found in the review by Etrich, Lederer, Malomed, Peschel and Peschel [2000] on solitons in various SHG media.

A different model based on resonant Bragg reflection and SHG nonlinearity can be formulated in the *spatial domain* [unlike the time-domain models (2.1) and (2.3)], for stationary fields in a planar (2D) nonlinear optical waveguide. In such a waveguide, a 1D Bragg grating is realized as a system of parallel scores ('scratches'). The simplest model of this type involves three waves (Mak, Malomed and Chu [1998b]):

$$i\frac{\partial\mathcal{E}_1}{\partial\zeta} + i\frac{\partial\mathcal{E}_1}{\partial x} + \mathcal{E}_2 + \mathcal{E}_3\mathcal{E}_2^* = 0, \quad (2.4a)$$

$$i\frac{\partial\mathcal{E}_2}{\partial\zeta} - i\frac{\partial\mathcal{E}_2}{\partial x} + \mathcal{E}_1 + \mathcal{E}_3\mathcal{E}_1^* = 0, \quad (2.4b)$$

$$2i\frac{\partial\mathcal{E}_3}{\partial\zeta} - q\mathcal{E}_3 + D\frac{\partial^2\mathcal{E}_3}{\partial x^2} + \mathcal{E}_1\mathcal{E}_2 = 0. \quad (2.4c)$$

Here ζ and x are the propagation and transverse coordinates, respectively; the fields \mathcal{E}_1 and \mathcal{E}_2 are two components of the fundamental harmonic that are transformed

into each other by resonant reflections on the 1D Bragg grating, \mathcal{E}_3 is the second-harmonic component, and D is an effective diffraction coefficient for the second harmonic. The wave vectors $\mathbf{k}_{1,2,3}$ of the three waves are related by the resonance condition, $\mathbf{k}_1 + \mathbf{k}_2 = \mathbf{k}_3$, the real parameter q accounts for a residual phase-mismatch. The configuration corresponding to this model assumes that the second harmonic propagates parallel to the Bragg grating (which has the form of the above-mentioned scores). It is therefore necessary to take into account the diffraction of this component, while for the two fundamental harmonics the effective diffraction induced by resonant Bragg scattering is much stronger than normal diffraction, which is neglected here.

The soliton spectrum of this model is fairly rich. It contains (Mak, Malomed and Chu [1998b]) not only fundamental single-humped solitons but also their two-humped bound states, some of which, as in the case of the four-wave model (2.3), may be dynamically stable. A rigorous stability analysis for various solitons in the model (2.4), based on computation of eigenvalues of the corresponding linearized equations, was performed by Schöllmann and Mayer [2000]. This analysis has shown that some of these solitons, although quite stable in direct dynamical simulations, are subject to a very weak oscillatory instability, whereas other solitons in this model are stable in the rigorous sense.

The three-wave model (2.4) possesses (Champneys and Malomed [2000]), besides the traditional GSs, numerous branches of *embedded solitons*: isolated solitary-wave solutions existing within the continuous spectrum, rather than inside the gap. Solutions of this kind appear also when the second-derivative terms are added to the generalized Thirring model (2.1).

Finally, the four-wave model (2.3) with quadratic nonlinearity can be extended to the two- and three-dimensional cases, by adding transverse diffraction terms to each equation of the system. Physically, this generalization corresponds to spatiotemporal evolution of the fields in a two- or three-dimensional layered medium. Because, as is well known, quadratic nonlinearity does not give rise to wave collapse in any number of physical dimensions, the latter model can support stable spatiotemporal solitons, frequently called *light bullets*. Direct numerical simulations reported by He and Drummond [1998] have confirmed the existence of stable ‘bullets’ in a multidimensional SHG medium embedded in a Bragg grating.

§ 3. Self-Induced Transparency (SIT) in Uniform Media and Thin Films

3.1. SIT IN UNIFORM MEDIA

Self-induced transparency (SIT) is the solitary propagation of electromagnetic (EM) pulses in near-resonant atomic media, irrespective of the carrier-frequency detuning from resonance. This striking effect, which is of paramount importance in nonlinear optics, was discovered by McCall and Hahn [1969], McCall and Hahn [1970]. If the pulse duration is much shorter than the transition (spontaneous-decay) lifetime (T_1) and dephasing time (T_2), then the leading edge of the pulse is absorbed, inverting the atomic population, while the remainder of the pulse causes atoms to emit stimulated light and thus return the energy to the field. When conditions for the process are met, it is found that a steady-state pulse envelope is established

and then propagates without attenuation at a velocity that may be considerably less than the phase velocity of light in the medium.

We start with the Hamiltonian for a single atom in the field,

$$\hat{H} = \frac{\hbar\omega_0}{2}\hat{w} - \mathbf{E} \cdot \hat{\mathbf{d}}, \quad (3.1)$$

where

$$\hat{w} \equiv |e\rangle\langle e| - |g\rangle\langle g|, \quad (3.2)$$

is the atomic inversion operator, ω_0 is the atomic transition frequency, $|g\rangle$ and $|e\rangle$ denote the atomic ground and excited states, respectively, \mathbf{E} is the electric field vector and $\hat{\mathbf{d}}$ is the atomic dipole-moment operator. We take the projection on the field direction, so that $\mathbf{E} \cdot \hat{\mathbf{d}} = E\hat{d}$, where

$$\hat{d} \equiv \frac{\mu}{2} (\hat{P} + \hat{P}^\dagger), \quad (3.3)$$

μ being the dipole moment matrix element (chosen real) and

$$\hat{P} \equiv 2 |g\rangle\langle e| \quad (3.4)$$

atomic polarization operator.

We express the electric field at a given point by means of the Rabi frequency Ω as

$$E = \frac{\hbar}{2\mu} (\Omega e^{-i\omega_c t} + \Omega^* e^{i\omega_c t}). \quad (3.5)$$

The Heisenberg equations of motion $d\hat{A}/dt = 1/(i\hbar) [\hat{A}, \hat{H}]$, for the atomic polarization and inversion operators (3.4),(3.2), yield the Bloch equations for their expectation values (c-numbers) P and w , respectively

$$\partial_t P(z, t) = w(z, t)\Omega - i(\omega_0 - \omega_{12})P, \quad (3.6a)$$

$$\partial_t w(z, t) = -\frac{1}{2} [P^*(z, t)\Omega + \text{c.c.}]. \quad (3.6b)$$

The Maxwell equations (Newell and Moloney [1992]) reduce in the rotating-wave and slow-varying approximations to

$$\left(\frac{c}{n_0} \frac{\partial}{\partial z} + \frac{\partial}{\partial t} \right) \Omega = \tau_0^{-2} P, \quad (3.7)$$

where

$$\tau_0 = \frac{n_0}{\mu} \sqrt{\frac{\hbar}{2\pi\omega_c \varrho_0}}, \quad (3.8)$$

is the cooperative resonant absorption time, ϱ_0 being the TLS density (averaged over z), and n_0 is the refraction index of the host media.

In the simplest case, when the driving field is in resonance with the atomic transition, $\omega_0 = \omega_c$, the Bloch equations (3.6) can be easily integrated and the Maxwell equation (3.7) then reduces to the sine-Gordon equation

$$\frac{\partial^2 \theta}{\partial \zeta \partial \tilde{\tau}} = -\sin \theta \quad (3.9)$$

for the ‘rotation angle’,

$$\theta = \int_{-\infty}^t \Omega dt', \quad (3.10)$$

in terms of the dimensionless variables $\tilde{\tau} = (t - n_0 z/c)/\tau_0$ and $\zeta = n_0 z/c\tau_0$.

This sine-Gordon equation is known to have solitary-wave solutions, for which the total area under the pulse is conserved and equal to 2π – the so called pulse-area theorem by McCall and Hahn [1969], McCall and Hahn [1970]:

$$\Omega(\zeta, \tilde{\tau}) = (\tau_0)^{-1} A_0 \operatorname{sech}[\beta(\zeta - v\tilde{\tau})], \quad (3.11)$$

where pulse width β is an arbitrary real parameter uniquely defining amplitude $A_0 = 2/\beta$ and group velocity $v = 1/\beta^2$ of the soliton.

Since its inception, SIT has become an active research area with many practical applications, for which we refer readers to excellent reviews by Lamb-Jr. [1971], Poluektov, Popov and Roitberg [1975], Maimistov, Basharov and Elyutin [1990] and references therein. In this section we will only briefly discuss results which are pertinent to the present review, such as SIT in thin films and collisions of counter-propagating SIT solitons.

3.2. SIT IN THIN FILMS

The interaction of light with a thin film of a nonlinear resonant medium located at the interface between two linear media has been described by Rupasov and Yudson [1982] and Rupasov and Yudson [1987], who have shown that a nonlinear thin film of TLS can be a nearly ideal mirror for weak pulses, but transparent for pulses of sufficient intensity. The problem of light pulse transmission through the nonlinear medium boundary has been studied under conditions of coherent interaction with the matter. The system can be described by a set of nonlinear Maxwell-Bloch-like equations which effectively take the presence of the reflected wave into account by imposing boundary conditions on the electromagnetic fields at the interface. It has been shown (Rupasov and Yudson [1987]) that these equations are exactly integrable by the inverse scattering method, and 2π -soliton-pulse transmission through the film has been studied.

If the atomic density is such that on average there are more than one atom per cubic resonant wavelength, then near-dipole-dipole (NDD) interactions, or local-field effects, can no longer be ignored, contrary to the case of more dilute media. NDD effects necessitate a correction to the field that couples to an atom in terms of the incident field and volume polarization (Bowden, Postan and Inguva [1991], Scalora and Bowden [1995]). This effect can give rise to *bistable optical transmission* of ultrashort light pulses through a thin layer consisting of two-level atoms (Basharov [1988], Benedict, Malyshev, Trifonov and Zaitsev [1991]): the local-field

correction leads to an inversion-dependent resonance frequency, and generates a new mechanism of nonlinear transparency. When the excitation frequency is somewhat larger than the original resonant frequency, the transmission of the layer exhibits a transient bistable behavior on the time scale of superradiance (Basharov [1988], Benedict, Malyshev, Trifonov and Zaitsev [1991]). It was shown that if an ultrashort pulse is allowed to interact with a thin film of optically dense two-level systems, the medium response is characterized by a rapid switching effect (Crenshaw, Scalora and Bowden [1992], Crenshaw and Bowden [1992]). This behavior is more remarkable than the response of conventional two-level systems, because the medium can only be found in one of two states: either fully inverted, or in the ground state, depending (quasi-periodically) on the ratio between the peak field-strength and the NDD coupling strength. This feature was found to be impervious to changes in pulse shape, and independent of the pulse area (Crenshaw, Scalora and Bowden [1992]).

Passage of light through a system of two thin TLS films of two-level atoms has been considered by Logvin and Samson [1992], Logvin and Loiko [2000] who have shown that if the distance between the films is an integer multiple of the wavelength, then the system is bistable. Self-pulsations, i.e., periodically generated output, arise if an odd number of half-wavelengths can be fitted between the films and absorption in the medium is insignificant. In general, the dynamics admits both regular and chaotic regimes.

3.3. COLLISIONS OF COUNTERPROPAGATING SIT SOLITONS

Situations in which it is necessary to consider the interaction of incident (forward) and reflected (backward) light waves include: intrinsic optical bistability (Inguva and Bowden [1990]), dynamics of excitations in a cavity (Shaw and Shore [1990]) and collisions of counterpropagating SIT solitons (Afanas'ev, Volkov, Dritz and Samson [1990], Shaw and Shore [1991]). The field in such problems is represented as a superposition of forward- and backward-traveling waves. The atomic response to this field is determined by solving the Bloch equations (3.6) in the rotating-wave approximation. The population inversion $w(z, t)$ and polarization P may be represented by a quasi-Fourier expansion over a succession of spatial harmonic carriers and slow varying envelopes, entangled in a fashion which leads to an *infinite hierarchy* of equations. *The truncation of this hierarchy can only be justified by phenomenological arguments*, such as atom movement in an active atomic gas.

When the forward (F-) and backward (B-) wave pulses overlap in space and time, the resulting interference pattern of nodes modifies the atomic excitation pattern. The spatial quasi-Fourier expansion provides an efficient way of treating the spatial inhomogeneities of the response in those regions where the F- and B-pulses overlap, each successive Rabi cycle increasing the number of terms that contribute to the expansion (Shaw and Shore [1990]).

Collisions of optical solitons produce observable effects on both the atoms and the pulses. The overlap of two counterpropagating pulses can produce an appreciable spatially-localized inversion of the atomic population, thus causing optical solitons to lose energy. It was found that, whereas large-energy solitons passed freely through each other, solitons whose initial energy fell below a critical value were destroyed by collisions. In addition, the residual atomic dipole, created by the

excitation, acts as a further source of radiation. This radiation appears as an oscillating tail on the postcollisional pulses and, over longer time scales, as fluorescence (Afanas'ev, Volkov, Dritz and Samson [1990], Shaw and Shore [1991]).

§ 4. SIT in Resonantly Absorbing Bragg Reflectors (RABR): The Model

4.1. MAXWELL EQUATIONS

Let us assume (Kozhekin and Kurizki [1995], Kozhekin, Kurizki and Malomed [1998], Opatrný, Malomed and Kurizki [1999]) a one-dimensional (1D) periodic modulation of the linear refractive index $n(z)$ along the z direction of the electromagnetic wave propagation (see Fig. 3). The modulation can be written as the Fourier series

$$n^2(z) = n_0^2[1 + a_1 \cos(2k_c z) + a_2 \cos(4k_c z) + \dots], \quad (4.1)$$

where n_0 , a_j and k_c are constants, and the medium is assumed to be infinite and homogeneous in the x and y directions.

The periodic grating gives rise to photonic band gaps (PBGs) in the system's linear spectrum, i.e., the medium is totally reflective for waves whose frequency is inside the gaps. The central frequency of the fundamental gap is $\omega_c = k_c c / n_0$, c being the vacuum speed of light, and the gap edges are located at the frequencies

$$\omega_{1,2} = \omega_c (1 \pm a_1/4), \quad (4.2)$$

where a_1 is the modulation depth from Eq. (4.1).

We further assume that *very thin* TLS layers (much thinner than $1/k_c$), whose resonance frequency ω_0 is close to the gap center ω_c , are placed at the maxima of the modulated refraction index. In other words, the thin active layers are placed at the points z_{layer} such that $\cos(k_c z_{\text{layer}}) = \pm 1$.

We shall study the propagation of electromagnetic waves with frequencies close to ω_c through the described medium. Let us write the Maxwell equation for one component of the field vector propagating in the z direction as

$$c^2 \frac{\partial^2 E}{\partial z^2} - n^2(z) \frac{\partial^2 E}{\partial t^2} = \frac{\partial^2 P_{nl}}{\partial t^2}, \quad (4.3)$$

with the refraction index n modulated as in Eq. (4.1), E being the electric field component and P_{nl} the non-linear polarization. We use the substitution

$$E \equiv [\mathcal{E}_F(z, t)e^{ik_c z} + \mathcal{E}_B(z, t)e^{-ik_c z}] e^{-i\omega_c t} + c.c., \quad (4.4)$$

with ω_c satisfying the dispersion relation $n_0 \omega_c = k_c c$ and \mathcal{E}_F and \mathcal{E}_B denoting the forward and backward propagating field components. We work in the slowly-varying envelope approximation

$$\left| \frac{\partial^2 \mathcal{E}_{B,F}}{\partial z^2} \right| \ll \left| k_c \frac{\partial \mathcal{E}_{B,F}}{\partial z} \right|, \quad (4.5a)$$

$$\left| \frac{\partial^2 \mathcal{E}_{B,F}}{\partial t^2} \right| \ll \left| \omega_c \frac{\partial \mathcal{E}_{B,F}}{\partial t} \right|. \quad (4.5b)$$

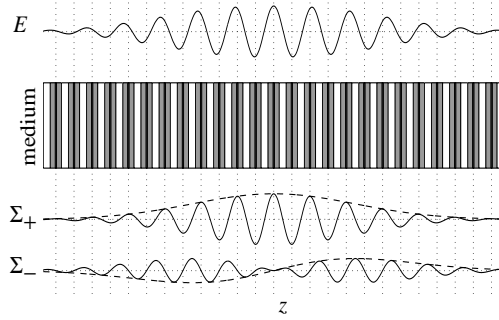


Figure 3: Schematic description of the periodic RABR and of the decomposition of the electric field into modes Σ_+ and Σ_- . The shading represents regions with different index of refraction; the darker the shading the larger n is. The black regions correspond to the TLS layers. The upper solid curve represents the electric field, the lower solid curves correspond to the components $\text{Re}(\Sigma_+)\cos k_c z$ and $-\text{Im}(\Sigma_-)\sin k_c z$; the dashed curves are the envelopes $\text{Re}(\Sigma_+)$ and $-\text{Im}(\Sigma_-)$. The vertical dotted lines denote the positions of the TLS.

Substituting (4.4) into (4.3), using (4.5a) and (4.5b), multiplying by $e^{i(\mp k_c z + \omega_c t)}$ and averaging over the wavelength $\lambda = 2\pi/k_c$ and the period $T = 2\pi/\omega_c$ we get

$$\frac{c}{n_0} \frac{\partial \mathcal{E}_F}{\partial z} + \frac{\partial \mathcal{E}_F}{\partial t} = \frac{ia_1 \omega_c}{4} \mathcal{E}_B + \frac{\hbar}{2\mu\tau_0^2} P_-, \quad (4.6a)$$

$$-\frac{c}{n_0} \frac{\partial \mathcal{E}_B}{\partial z} + \frac{\partial \mathcal{E}_B}{\partial t} = \frac{ia_1 \omega_c}{4} \mathcal{E}_F + \frac{\hbar}{2\mu\tau_0^2} P_+, \quad (4.6b)$$

where we define

$$P_{\pm} \equiv -\frac{i\mu\tau_0^2}{\hbar\omega_c n_0^2} \left\langle \frac{\partial^2 P_{nl}}{\partial t^2} e^{i(\pm k_c z + \omega_c t)} \right\rangle_{\lambda, T}, \quad (4.7)$$

with μ being the dipole moment (Ch.3, and τ_0 a constant chosen here to be the medium absorption time [see Eq. (3.8)]. The averaging is defined as

$$\langle \dots \rangle_{\lambda, T} \equiv \frac{1}{\lambda T} \int_{\lambda} \int_T \dots dt dz. \quad (4.8)$$

We express the field components $\mathcal{E}_{F,B}$ by means of the dimensionless quantities Σ_{\pm} ,

$$\mathcal{E}_{F,B} = \frac{\hbar}{4\mu\tau_0} (\Sigma_+ \pm \Sigma_-), \quad (4.9)$$

so that the electric field $E = E(z, t)$ is

$$E(z, t) = \hbar(\mu\tau_0)^{-1} \left(\text{Re} [\Sigma_+(z, t)e^{-i\omega_c t}] \cos k_c z - \text{Im} [\Sigma_-(z, t)e^{-i\omega_c t}] \sin k_c z \right). \quad (4.10)$$

To obtain the equations of motion in the most compact form, it is convenient to introduce the dimensionless time τ , coordinate ζ , and detuning δ as

$$\tau \equiv t/\tau_0, \quad \zeta \equiv (n_0/c\tau_0) z, \quad \delta \equiv (\omega_0 - \omega_c)\tau_0, \quad (4.11)$$

where τ_0 is the *characteristic absorption time* of the field by the TLS medium as defined by Eq. (3.8). Substituting Eq. (4.9) into (4.6a) and (4.6b), using (4.11) and (3.8), then differentiating the equations again with respect to ζ and τ , we arrive, after algebra, at the form

$$\begin{aligned} \frac{\partial^2 \Sigma_+}{\partial \tau^2} - \frac{\partial^2 \Sigma_+}{\partial \zeta^2} &= -\eta^2 \Sigma_+ + i\eta(P_+ + P_-), \\ &+ \frac{\partial}{\partial \tau}(P_+ + P_-) + \frac{\partial}{\partial \zeta}(P_+ - P_-), \end{aligned} \quad (4.12a)$$

and

$$\begin{aligned} \frac{\partial^2 \Sigma_-}{\partial \tau^2} - \frac{\partial^2 \Sigma_-}{\partial \zeta^2} &= -\eta^2 \Sigma_- + i\eta(P_+ - P_-) \\ &- \frac{\partial}{\partial \tau}(P_+ - P_-) - \frac{\partial}{\partial \zeta}(P_+ + P_-). \end{aligned} \quad (4.12b)$$

Here the dimensionless modulation strength η is the ratio of the TLS *absorption distance* $l_{\text{abs}} = \tau_0 c/n_0$ to the *Bragg reflection distance* $l_{\text{refl}} = 4c/(a_1 \omega_c n_0)$, which can be expressed as

$$\eta = l_{\text{abs}}/l_{\text{refl}} = a_1 \omega_c \tau_0 / 4. \quad (4.13)$$

The equations for the electric field components Σ_{\pm} can be solved once we know the averaged polarization P_{\pm} . To find P_{\pm} , we express the polarization P_{nl} at a given point as the dipole moment density

$$\begin{aligned} P_{nl} &= 4\pi \varrho \langle d \rangle = 2\pi \varrho \mu \left(\langle \hat{P} \rangle + \langle \hat{P}^\dagger \rangle \right) \\ &= -2\pi i \varrho \mu \left(P e^{-i\omega_c t} - P^* e^{i\omega_c t} \right), \end{aligned} \quad (4.14)$$

where ϱ is the number of the two-level atoms in a unit volume. Neglecting the time derivatives of P with respect to those of $e^{-i\omega_c t}$, we can write for the polarization derivative

$$\frac{\partial^2 P_{nl}}{\partial t^2} = 2\pi i \omega_c^2 \varrho \mu \left(P e^{-i\omega_c t} - P^* e^{i\omega_c t} \right), \quad (4.15)$$

so that P_{\pm} on the right-hand side of Eqs. (4.6a), (4.6b) read as

$$P_{\pm} = \frac{2\pi \omega_c^2 \mu^2 \tau_0^2}{\hbar n_0^2} \langle \varrho P e^{\pm i k_c z} \rangle_{\lambda}. \quad (4.16)$$

To determine the evolution of P_{\pm} , we have to make certain approximations. Let us first consider the situation when the TLS's are confined to *infinitely thin* layers. We will subsequently study the influence of finite width of the layers.

4.2. TWO-LEVEL SYSTEMS (TLS) IN INFINITELY THIN LAYERS

Let us now assume that the atomic density ϱ is concentrated in zero-width layers located at z_j such that

$$e^{i k_c z_{2j}} = 1, \quad e^{i k_c z_{2j+1}} = -1 \quad (4.17)$$

i.e., it is described by

$$\varrho = \frac{\varrho_0 \lambda}{2} \sum_j \delta(z - z_j), \quad (4.18)$$

where ϱ_0 is the bulk density averaged over the whole wavelength. We also assume that the spatial dependence of P is to a good approximation *anti-periodic* with respect to $\lambda/2$, i.e. $P(z+\lambda/2) \approx -P(x)$. This is in agreement with the approximate anti-periodicity of the electric field with $\lambda/2$. Denoting by P_0 the value of P in even-numbered layers (the value in the odd-numbered layer being $-P_0$), we get the spatial average in (4.16) as

$$P_{\pm} = \frac{2\pi\omega_c\mu^2\varrho_0\tau_0^2}{\hbar m_0^2} P_0. \quad (4.19)$$

Note that $P_+ = P_-$ is the consequence of the zero width of the layers. Due to the choice of τ_0 as in Eq. (3.8), we obtain the simple relation

$$P_{\pm} = P_0. \quad (4.20)$$

Using this expression in (4.12a) and (4.12b), we obtain the following evolution equations for Σ_{\pm}

$$\frac{\partial^2 \Sigma_+}{\partial \tau^2} - \frac{\partial^2 \Sigma_+}{\partial \zeta^2} = -\eta^2 \Sigma_+ + 2i\eta P + 2\frac{\partial P}{\partial \tau}, \quad (4.21a)$$

$$\frac{\partial^2 \Sigma_-}{\partial \tau^2} - \frac{\partial^2 \Sigma_-}{\partial \zeta^2} = -\eta^2 \Sigma_- - 2\frac{\partial P}{\partial \zeta}, \quad (4.21b)$$

where we have omitted the index 0 of P_0 , for simplicity.

The equations for the polarization P and inversion w in the even-numbered layers can be obtained from Eqs. (3.6) by substituting for Ω (combining Eqs. (4.10) and (3.5))

$$\Omega = \tau_0^{-1} (\Sigma_+ \cos k_c z + i\Sigma_- \sin k_c z) \quad (4.22)$$

and applying Eq. (4.17) at the positions of these layers. Expressing the detuning as in Eq. (4.11), we obtain the equations

$$\frac{\partial P}{\partial \tau} = -i\delta P + \Sigma_+ w, \quad (4.23a)$$

$$\frac{\partial w}{\partial \tau} = -\text{Re} (\Sigma_+ P^*). \quad (4.23b)$$

The set of equations (4.21) and (4.23) was first derived by Mantsyzov and Kuz'min [1984] and Mantsyzov and Kuz'min [1986] for the particular case of a periodic array of thin TLS layers *without* modulation of the linear index of refraction, i.e., $\eta = 0$. In this case, these equations can be reduced to the sine-Gordon equation (3.9) for the area of the 'forward' wave

$$\Psi(z, t) = \int_{-\infty}^t \Sigma_+(z, t') dt'. \quad (4.24)$$

It follows from (4.24) that the 2π solitary wave (SIT), associated with the sum of the forward and backward propagating waves, is an *exact* solution to the coupled-mode Maxwell-Bloch equations for a periodic stack of resonant thin films satisfying the Bragg condition. These solitary wave solutions are referred to as “two-wave solitons” (Mantsyzov and Kuz'min [1986]).

If the Bragg condition is not exactly satisfied, then the system can exhibit a rich, multi-stable behavior, which has been studied numerically (Mantsyzov [1992], Lakoba and Mantsyzov [1992], Lakoba [1994]). In the case of a slight violation of the Bragg condition at the exact two-level resonance, an analytical solution for the 2π gap soliton with a phase modulation had been obtained (Mantsyzov [1995]). These studies have also revealed the existence of an oscillating pulse, whose amplitude and velocity sign change periodically.

Combining Eqs. (4.23a) and (4.23b), one can eliminate the TLS population inversion:

$$w = \pm \sqrt{1 - |P|^2}. \quad (4.25)$$

Without the field-induced polarization, the TLS population is not inverted ($w = -1$), hence the lower sign must be chosen in Eq. (4.25). Thus, the remaining equations for Σ_+ and P form a *closed system*,

$$\frac{\partial^2 \Sigma_+}{\partial \tau^2} - \frac{\partial^2 \Sigma_+}{\partial \zeta^2} = - \eta^2 \Sigma_+ + 2i(\eta - \delta)P - 2\sqrt{1 - |P|^2} \Sigma_+, \quad (4.26a)$$

$$\frac{\partial P}{\partial \tau} = - i\delta P - \sqrt{1 - |P|^2} \Sigma_+, \quad (4.26b)$$

and Σ_- , the field component driven by $\partial P / \partial \zeta$, can then be found from Eq. (4.21b).

4.3. FINITE WIDTH OF TLS LAYERS

So far, we have assumed that the TLS layers are infinitesimally thin. We now proceed to estimate effects of non-zero width of the active layers, which represent more realistic physical situations. We still assume the width of the active layers to be small in comparison to the wavelength. This allows us to expand the polarization as a Taylor series in the position within the layer, and consider only terms up to the second order. Averaging the polarization over the entire wavelength yields the source term of the Maxwell equations (4.6).

Let us assume that the TLS density is given, instead of Eq. (4.18), by

$$\varrho = \frac{\varrho_0 \lambda}{2} f(x), \quad (4.27)$$

where ϱ_0 is the density averaged over the whole wavelength and the function $f(z)$

has the properties

$$\begin{aligned}
f(z) \geq 0, \quad f(z + \lambda/2) &= f(z), \\
\int_{z_j - \frac{\lambda}{4}}^{z_j + \frac{\lambda}{4}} f(z) dz &= 1, \\
\int_{z_j - \frac{\lambda}{4}}^{z_j + \frac{\lambda}{4}} z f(z) dz &= 0, \\
\int_{z_j - \frac{\lambda}{4}}^{z_j + \frac{\lambda}{4}} z^2 f(z) dz &= \frac{\gamma^2}{k^2},
\end{aligned} \tag{4.28}$$

where $\gamma \ll 1$ is a dimensionless parameter describing the thickness of the layers. For a rectangular function f of width D this parameter is

$$\gamma = \frac{\pi D}{\sqrt{3}\lambda}. \tag{4.29}$$

To calculate $\langle \varrho P e^{\pm i k_c z} \rangle_\lambda$ of (4.16), we expand the spatial dependence of P and $\exp(\pm i k_c z)$ in Taylor series,

$$\begin{aligned}
\langle \varrho P e^{\pm i k_c z} \rangle_\lambda &= e^{\pm i k_c z_{2j}} \varrho_0 \int_{z_{2j} - \frac{\lambda}{4}}^{z_{2j} + \frac{\lambda}{4}} f(z) \\
&\times \left[P_0 + P'_0(z - z_{2j}) + \frac{1}{2} P''_0(z - z_{2j})^2 + \dots \right] \\
&\times \left[1 \pm i k_c(z - z_{2j}) - \frac{k_c^2}{2}(z - z_{2j})^2 + \dots \right] dz,
\end{aligned} \tag{4.30}$$

where P_0 , P'_0 , and P''_0 refer to the values of P and its spatial first and second derivatives at the positions of the even-numbered layers. Neglecting higher than quadratic terms and using Eqs. (4.28), we arrive at

$$\langle \varrho P e^{\pm i k_c z} \rangle_\lambda \approx \varrho_0 \left[P_0 + \gamma^2 \left(\frac{P''_0}{2k^2} \pm \frac{iP'_0}{k} - \frac{P_0}{2} \right) \right], \tag{4.31}$$

so that

$$P_\pm \approx P_0 + \gamma^2 \left(\frac{P''_0}{2k^2} \pm \frac{iP'_0}{k} - \frac{P_0}{2} \right). \tag{4.32}$$

Using these values in (4.16), substituting them into (4.12a) and (4.12b), and defining

$$P_0 \equiv P(z_{2j}), \tag{4.33}$$

$$P_B \equiv -\frac{2i}{k} \frac{\partial P}{\partial z} \Big|_{z=z_{2j}}, \tag{4.34}$$

$$P_C \equiv \left(\frac{1}{k^2} \frac{\partial^2}{\partial z^2} - 1 \right) P \Big|_{z=z_{2j}}, \tag{4.35}$$

we obtain the field equations of motion in the form

$$\begin{aligned} \frac{\partial^2 \Sigma_+}{\partial \tau^2} - \frac{\partial^2 \Sigma_+}{\partial \zeta^2} &= -\eta^2 \Sigma_+ + 2i\eta P_0 + 2\frac{\partial P_0}{\partial \tau} \\ &+ \gamma^2 \left[i\eta P_C + \frac{\partial P_C}{\partial \tau} - \frac{\partial P_B}{\partial \zeta} \right], \end{aligned} \quad (4.36a)$$

$$\begin{aligned} \frac{\partial^2 \Sigma_-}{\partial \tau^2} - \frac{\partial^2 \Sigma_-}{\partial \zeta^2} &= -\eta^2 \Sigma_- - 2\frac{\partial P_0}{\partial \zeta} \\ &+ \gamma^2 \left[-i\eta P_B - \frac{\partial P_C}{\partial \zeta} - \frac{\partial P_B}{\partial \tau} \right]. \end{aligned} \quad (4.36b)$$

To obtain the equations of motion for the atomic parameters, we use Eq. (4.22) for Ω in (3.6) and rewrite the Bloch equations at a point z as

$$\frac{\partial P}{\partial \tau} = -i\delta P + [\cos(k_c z)\Sigma_+ + i\sin(k_c z)\Sigma_-] w, \quad (4.37a)$$

$$\frac{\partial w}{\partial \tau} = -\frac{1}{2} [\cos(k_c z)\Sigma_+ + i\sin(k_c z)\Sigma_-] P^* + \text{c.c.} \quad (4.37b)$$

Considering that the spatial derivatives of Σ_{\pm} are much smaller than those of $\sin(k_c z)$ and $\cos(k_c z)$, and calculating the first and second derivatives at the positions of the even-numbered layers, we get

$$\frac{\partial P_0}{\partial \tau} = -i\delta P_0 + \Sigma_+ w_0, \quad (4.38)$$

$$\frac{\partial P'_0}{\partial \tau} = -i\delta P'_0 + ik_c \Sigma_- w_0 + \Sigma_+ w'_0, \quad (4.39)$$

$$\frac{\partial P''_0}{\partial \tau} = -i\delta P''_0 - k_c^2 \Sigma_+ w_0 + 2ik_c \Sigma_- w'_0 + \Sigma_+ w''_0, \quad (4.40)$$

and

$$\frac{\partial w_0}{\partial \tau} = -\frac{1}{2} \Sigma_+ P_0^* + \text{c.c.}, \quad (4.41)$$

$$\frac{\partial w'_0}{\partial \tau} = -\frac{ik_c}{2} \Sigma_- P_0^* - \frac{1}{2} \Sigma_+ P_0^* + \text{c.c.}, \quad (4.42)$$

$$\frac{\partial w''_0}{\partial \tau} = \frac{k_c^2}{2} \Sigma_+ P_0^* - ik_c \Sigma_- P_0^* - \frac{1}{2} \Sigma_+ P_0^* + \text{c.c.} \quad (4.43)$$

Using the definitions (4.33) – (4.35) and defining

$$w_0 \equiv w(z_{2j}), \quad (4.44)$$

$$w_1 \equiv \left. \frac{i}{k} \frac{\partial w}{\partial z} \right|_{z=z_{2j}}, \quad (4.45)$$

$$w_2 \equiv \left. \left(\frac{1}{k^2} \frac{\partial^2}{\partial z^2} - 2 \right) w \right|_{z=z_{2j}}, \quad (4.46)$$

we then arrive at the equations of motion

$$\frac{\partial P_0}{\partial \tau} = -i\delta P_0 + w_0 \Sigma_+, \quad (4.47)$$

$$\frac{\partial P_B}{\partial \tau} = -i\delta P_B + 2w_0 \Sigma_- - 2w_1 \Sigma_+, \quad (4.48)$$

$$\frac{\partial P_C}{\partial \tau} = -i\delta P_C + w_2 \Sigma_+ + 2w_1 \Sigma_-, \quad (4.49)$$

$$\frac{\partial w_0}{\partial \tau} = -\frac{1}{2} \Sigma_+ P_0^* + \text{c.c.}, \quad (4.50)$$

$$\frac{\partial w_1}{\partial \tau} = \frac{1}{2} \Sigma_- P_0^* - \frac{1}{4} \Sigma_+ P_B^* - \text{c.c.}, \quad (4.51)$$

$$\frac{\partial w_2}{\partial \tau} = \Sigma_+ \left(P_0^* - \frac{1}{2} P_C^* \right) - \frac{1}{2} \Sigma_- P_B^* + \text{c.c.} \quad (4.52)$$

Equations (4.36a), (4.36b) and (4.47) – (4.49) with their complex conjugates and Eqs. (4.50) – (4.52) form a closed set of 13 equations for the variables Σ_+ , Σ_- , P_0 , P_B , P_C and their complex conjugates and w_0 , w_1 and w_2 , i.e., 13 real variables together. The equations are parametrized by 3 real parameters η , δ and γ . Note that for $\gamma = 0$ Eqs. (4.36a), (4.36b), (4.47) and (4.50) are identical to Eqs. (4.21a), (4.21b), (4.23a) and (4.23b), respectively, with P_0 standing for P . Even though the number of equations and variables has now increased, they are still relatively easy to solve numerically, and can realistically express the properties of the system over rather long times.

The case of a *uniform active medium* embedded in a Bragg grating calls either for a solution of the *full second-order Maxwell equation*, without the spatial slow varying approximation, or for a solution of an *infinite set of coupled equations* for P_i and w_i as in the case discussed in Ch.3.3. This makes the *present analysis principally at variance* with that of Aközbeke and John [1998], where the slow varying approximation for atomic inversion and polarization is assumed, thus *arbitrarily truncating* the infinite hierarchy of equations to its first two orders.

4.4. ENERGY DENSITIES

To reveal the physical meaning of the quantities Σ_{\pm} and P , we express the energy density of the electromagnetic field as

$$W_F = (1/8) \hbar \omega_c \rho_0 (|\Sigma_+|^2 + |\Sigma_-|^2), \quad (4.53)$$

that of the TLS excitations (considering the limit of infinitely thin TLS layers) as

$$W_A = (1/2) \hbar \omega_0 \rho_0 \left(1 - \sqrt{1 - |P|^2} \right), \quad (4.54)$$

and the energy density of the TLS-field interaction as

$$W_I = (1/2) \hbar \rho_0 \tau_0^{-1} \text{Im} (\Sigma_+ P^*). \quad (4.55)$$

From Eq. (4.53) we conclude that $|\Sigma_+|^2$ and $|\Sigma_-|^2$ are proportional to the number of photons per TLS (atom), in the standing-wave symmetric and anti-symmetric

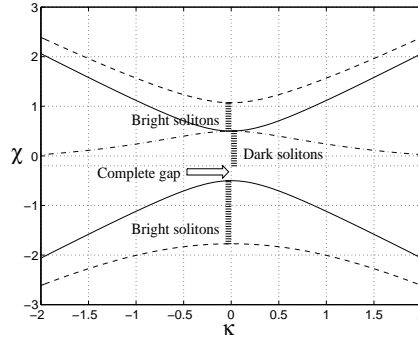


Figure 4: The RABR dispersion curves (dimensionless frequency χ versus dimensionless wavevector k) at $\eta = 0.5$ and $\delta = -0.2$. The solid lines show the dispersion branches corresponding to the ‘bare’ (noninteracting) grating, while the dashed and dash-dotted lines stand for the dispersion branches of the grating ‘dressed’ by the active medium. The frequency bands that support the standing dark and bright solitons are shaded. The arrow indicates a complete gap, where no field propagation of any kind can take place.

modes, whose anti-nodes and nodes, respectively, coincide with the active layers (see Fig. 3). Since the interaction time τ_0 (see Eq. (3.8)) is usually much larger than the optical period $2\pi/\omega_c$, the interaction energy is negligible in comparison with the energies of the field and atomic excitations.

4.5. LINEARIZED SPECTRUM

To reach general understanding of the dynamics of the model, the first necessary step is to consider the spectrum produced by the linearized version of Eqs. (4.21b), (4.26a) and (4.26b), which describe *weak fields* in the limit of infinitely thin TLS layers. Setting $w = -1$, and

$$\Sigma_+ = Ae^{i(\kappa\zeta - \chi\tau)}, \quad (4.56a)$$

$$\Sigma_- = Be^{i(\kappa\zeta - \chi\tau)}, \quad (4.56b)$$

$$P = Ce^{i(\kappa\zeta - \chi\tau)}, \quad (4.56c)$$

we obtain from the linearized equation (4.26b) that $C = i(\delta - \chi)^{-1}A$. Substituting this into Eqs.(4.21b) and (4.26a), we arrive at the dispersion relation for the wavenumber κ and frequency χ in the form

$$(\chi^2 - \kappa^2 - \eta^2)(\chi - \delta) \times \{(\chi - \delta) [\chi^2 - \kappa^2 - (2 + \eta^2)] + 2(\eta - \delta)\} = 0. \quad (4.57)$$

Different branches of the dispersion relation generated by Eq. (4.57) are shown in Fig. 4. The roots $\chi = \pm\sqrt{\kappa^2 + \eta^2}$ (corresponding to the solid lines in Fig. 4) originate from the driven equation (4.21b) and represent the dispersion relation of the Bragg reflector with the gap $|\chi| < \eta$ (cf. Eq. (4.2)), that does not feel the interaction with the active layers. The degenerate root $\chi \equiv \delta$ is trivial, as it corresponds to the eigenmode (4.56c) with $A = B = 0$. Important roots are those

given by the curly brackets in Eq. (4.57) (shown by the dashed and dash-dotted lines in Fig. 3), since they give rise to nontrivial spectral features. They will be shown below to correspond to bright or dark solitons in the indicated (shaded) bands.

The frequencies corresponding to $k = 0$ are

$$\chi_0 = \eta \text{ and } \chi_{0,\pm} = -\frac{1}{2}(\eta - \delta) \pm \sqrt{2 + \frac{1}{4}(\eta + \delta)^2}, \quad (4.58)$$

while at $k^2 \rightarrow \infty$ the asymptotic expressions for different branches of the dispersion relation are $\chi = \pm k$ and $\chi = \delta + 2(\eta - \delta)k^{-2}$. Thus, the linearized spectrum always splits into *two gaps*, separated by an allowed band, except for the special case, $\eta = \eta_0 \equiv \frac{1}{2}\delta + \sqrt{1 + \frac{1}{4}\delta^2}$, when the upper gap closes down. The upper and lower band edges are those of the periodic structure, shifted by the induced TLS polarization in the limit of a strong reflection. They approach the SIT spectral gap for forward- and backward-propagating waves (Mantsyzov [1995]) in the limit of weak reflection. The allowed middle band corresponds to a polaritonic (collective atomic polarization) excitation in the periodic structure. It is different from single-photon hopping in a PBG via resonant dipole-dipole interactions (John and Quang [1995]).

§ 5. Bright Solitons in RABR

5.1. STANDING (QUIESCENT) SELF-LOCALIZED PULSES

Stationary solutions of Eqs. (4.26a) and (4.26b) corresponding to bright solitons have been found by Kozhekin, Kurizki and Malomed [1998]. Such solutions for the symmetric-mode field Σ_+ and polarization P are sought in the form

$$\Sigma_+ = e^{-i\chi\tau} \mathcal{S}(\zeta), \quad P = i e^{-i\chi\tau} \mathcal{P}(\zeta) \quad (5.1)$$

with real \mathcal{P} and \mathcal{S} . Substituting this into (4.26b), we eliminate \mathcal{P} in favor of \mathcal{S} ,

$$\mathcal{P} = -\frac{\text{sign}(\chi - \delta) \cdot \mathcal{S}}{\sqrt{(\chi - \delta)^2 + |\mathcal{S}|^2}}, \quad (5.2)$$

and obtain an equation for $\mathcal{S}(\zeta)$,

$$\mathcal{S}'' = (\eta^2 - \chi^2)\mathcal{S} - 2\mathcal{S} \frac{(\eta - \chi) \cdot \text{sign}(\chi - \delta)}{\sqrt{(\chi - \delta)^2 + \mathcal{S}^2}}, \quad (5.3)$$

where the prime stands for $d/d\zeta$. Equation (5.3) can be cast into the form of the Newton's equation of motion for a particle with the coordinate $\mathcal{S}(\zeta)$ moving in a potential $U(\mathcal{S})$:

$$\mathcal{S}'' = -U'(\mathcal{S}), \quad (5.4)$$

where

$$U(\mathcal{S}) = -\frac{1}{2}(\eta^2 - \chi^2)\mathcal{S}^2 + 2(\eta - \chi) \cdot \text{sign}(\chi - \delta) \sqrt{(\chi - \delta)^2 + \mathcal{S}^2}. \quad (5.5)$$

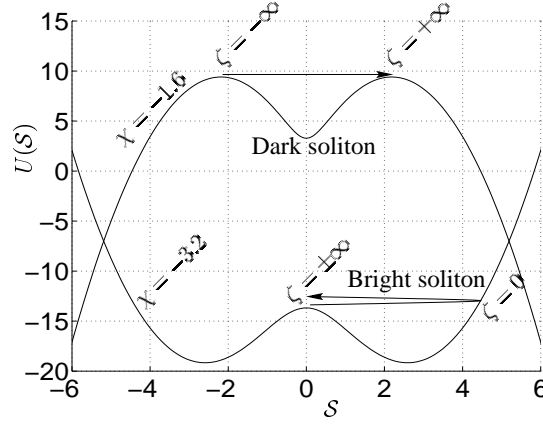


Figure 5: The potentials $U(\mathcal{S})$ of Eq. (5.5) leading to the bright ($\chi = -3.2$) and dark ($\chi = -1.6$) standing solitons. The system parameters are $\delta = -2$, and $\eta = 2.5$.

The potential gives rise to bright solitons (Newell and Moloney [1992]), provided it has two symmetric minima (see Fig. 5). As follows from Eq. (5.5), the latter condition implies that the quadratic part of the potential is concave, i.e., $|\chi| > \eta$, and the second (asymptotically linear) part of the expression (5.5) is convex, so that $\chi < \delta$. Moreover, two minima separated by a local maximum in $\mathcal{S} = 0$ appear if $U''(0) < 0$. From this inequality it follows that bright solitons can appear in two frequency bands χ , the lower band

$$\chi_1 < \chi < \min\{\chi_2, -\eta, \delta\}, \quad (5.6)$$

and the upper band

$$\max\{\chi_1, \eta, \delta\} < \chi < \chi_2, \quad (5.7)$$

where the boundary frequencies $\chi_{1,2}$ are given by

$$\chi_{1,2} \equiv (1/2) \left[\delta - \eta \mp \sqrt{(\eta + \delta)^2 + 8} \right]. \quad (5.8)$$

The lower band exists for all values $\eta > 0$ and δ , while the upper one only exists for

$$\delta > \eta - 1/\eta, \quad (5.9)$$

which follows from the requirement $\chi_2 > \eta$ (see Eq. (5.7)). On comparing these expressions with the spectrum shown in Fig. 4, we conclude that part of the lower gap is always empty from solitons, while the upper gap is completely filled with stationary solitons in the weak-reflectivity case (5.9), and completely empty in the opposite limit. It is relevant to mention that a partly empty gap has also been found in a Bragg grating with second harmonic generation (Peschel, Peschel, Lederer and Malomed [1997]), see Ch. 2.

The bright soliton corresponds to the solution of the Newton equation (5.4) with the ‘particle’ sitting at time $-\infty$ on the local maximum $\mathcal{S} = 0$, then swinging to one side and finally returning to $\mathcal{S} = 0$ at time $+\infty$. Such solutions have been found in an implicit form by Kozhokin, Kurizki and Malomed [1998]:

$$\mathcal{S}(\zeta) = 2|\chi - \delta|\mathcal{R}(\zeta) (1 - \mathcal{R}^2(\zeta))^{-1}, \quad (5.10)$$

with

$$|\zeta| = \sqrt{2 \left| \frac{\chi - \delta}{\chi - \eta} \right|} \left[(1 - \mathcal{R}_0^2)^{-1/2} \tan^{-1} \sqrt{\frac{\mathcal{R}_0^2 - \mathcal{R}^2}{1 - \mathcal{R}_0^2}} + (2\mathcal{R}_0)^{-1} \ln \left(\frac{\mathcal{R}_0 + \sqrt{\mathcal{R}_0^2 - \mathcal{R}^2}}{\mathcal{R}} \right) \right], \quad (5.11)$$

and

$$\mathcal{R}_0^2 = 1 - \frac{|(\chi + \eta)(\chi - \delta)|}{2} \quad (5.12)$$

(note that \mathcal{R}_0^2 is positive under the above conditions (5.6)-(5.9)). It can be checked that this zero-velocity (ZV) gap soliton is always *single*-humped. Its amplitude can be found from Eq. (5.11),

$$\mathcal{S}_{\max} = 4\mathcal{R}_0/\sqrt{|\chi + \eta|}. \quad (5.13)$$

The polarization amplitude \mathcal{P} is determined by \mathcal{S} via Eq. (5.2).

To calculate the electric field in the antisymmetric Σ_- mode, we substitute

$$\Sigma_- = ie^{-i\chi\theta} \mathcal{A}(\zeta) \quad (5.14)$$

into Eq. (4.21b) and obtain

$$\mathcal{A}'' + (\chi^2 - \eta^2) \mathcal{A} = 2\mathcal{P}', \quad (5.15)$$

which can be easily solved by the Fourier transform, once $\mathcal{P}(\zeta)$ is known. An example of bright solitons is depicted in Fig. 6. Note that, depending on the parameters η , δ and χ , the main part of the soliton energy can be carried either by the Σ_+ or the Σ_- mode.

The most drastic difference of these new solitons from the well-known SIT pulses is that the area of the ZV soliton is not restricted to 2π , but, instead, may take an *arbitrary* value. As mentioned above, this basic new result shows that the Bragg reflector can enhance (by multiple reflections) the field coupling to the TLS, so as to make the pulse area *effectively* equivalent to 2π . In the limit of the small-amplitude and small-area solitons, $\mathcal{R}_0^2 \ll 1$, Eq. (5.11) can be easily inverted, the ZV soliton becoming a broad sech-like pulse:

$$\mathcal{S} \approx 2|\chi - \delta|\mathcal{R}_0 \operatorname{sech} \left(\sqrt{2 \left| \frac{\chi - \eta}{\chi - \delta} \right|} \mathcal{R}_0 \zeta \right). \quad (5.16)$$

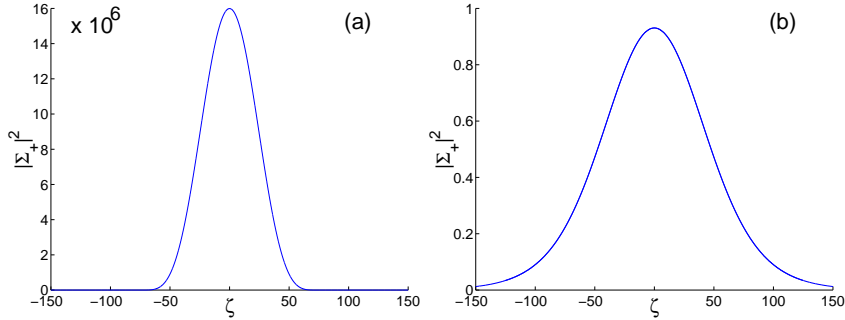


Figure 6: Zero-velocity (RABR) solitons $|\Sigma_+(\zeta)|^2$ (a) $\delta = 0$, $\eta = 0.9$, $\chi = -0.901$ (divergent width and amplitude); (b) idem, but for $\chi = 0.901$ (divergent width and finite amplitude).

In the opposite limit, $1 - \mathcal{R}_0^2 \rightarrow 0$, i.e., for vanishingly small $|\chi + \eta|$, the soliton's amplitude (5.13) becomes very large, and further analysis reveals that, in this case, the soliton is characterized by a *broad central part* with a width $\sim (1 - \mathcal{R}_0^2)^{-1/2}$ (Fig. 6(a)). Another special limit is $\chi - \eta \rightarrow 0$. It can be checked that in this limit, the amplitude (5.13) remains finite, but the *soliton width diverges* as $|\chi - \eta|^{-1/2}$ (Fig. 6(b)). Thus, although the ZV soliton has a single hump, its shape is, in general, strongly different from that of the traditional nonlinear-Schrödinger (NLS) sech pulse.

5.1.1. Stability

The stability of the ZV gap solitons was tested numerically, by means of direct simulations of the full system (4.26), the initial condition taken as the exact soliton with a small perturbation added to it. Simulations at randomly chosen values of the parameters, have invariably shown that the ZV GS are apparently *stable*. However, the possibility of their dynamical and structural instability needs be further investigated, as has been done in the case of GS in a Kerr-nonlinear fiber with a grating by Barashenkov, Pelinovsky and Zemlyanaya [1998] and Schöllmann and Mayer [2000].

5.2. MOVING SOLITONS

Although the system of Eqs. (4.26) is not explicitly Galilean- or Lorentz-invariant, translational invariance is expected on physical grounds. Hence, a full family of soliton solutions should have velocity as one of its parameters. This can be explicitly demonstrated in the limit of the small-amplitude large-width solitons [cf. Eq. (5.16)]. We search for the corresponding solutions in the form $\Sigma_+(\zeta, \tau) = \mathcal{S}(\zeta, \tau) \exp(-i\chi_0\tau)$, $P(\zeta, \tau) = i\mathcal{P}(\zeta, \tau) \exp(-i\chi_0\tau)$ (cf. Eqs. (5.1)), where χ_0 is the frequency corresponding to $k = 0$ on any of the three branches of the dispersion relation (4.58) (see Fig. 4), and the functions $\mathcal{S}(\zeta, \tau)$ and $\mathcal{P}(\zeta, \tau)$ are assumed to be slowly varying in comparison with $\exp(-i\chi_0\tau)$. Under these assumptions, we

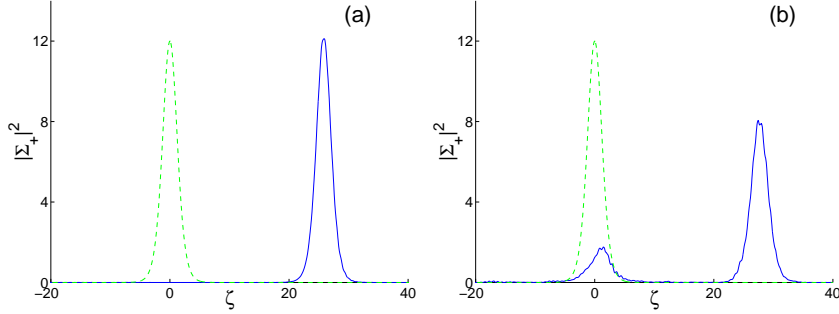


Figure 7: Pulses obtained as a result of ‘pushing’ a zero-velocity RABR soliton (dashed lines): (a) push, characterized by the initial multiplier $\exp(-ip\zeta)$ after a sufficiently long evolution ($\tau = 400$) (solid lines). $\delta = 0$, $\eta = 4$, $\chi = -4.4$, and $p = 0.1$. (b) idem, but for $p = 0.5$.

arrive at the following asymptotic equation for $\mathcal{S}(\zeta, \tau)$:

$$\left[2i \frac{\chi_0(\chi_0 - \delta)^2 - \eta + \delta}{(\chi_0 - \delta)^2} \frac{\partial}{\partial \tau} + \frac{\partial^2}{\partial \zeta^2} + \frac{\chi_0 - \eta}{(\chi_0 - \delta)^3} |\mathcal{S}|^2 \right] \mathcal{S} = \left(\eta^2 - \chi_0^2 + 2 \frac{\chi_0 - \eta}{\chi_0 - \delta} \right) \mathcal{S}. \quad (5.17)$$

Since this equation is of the NLS form, it has the full two-parameter family of soliton solutions, including the moving ones (Newell and Moloney [1992]).

In order to check the existence and stability of the moving solitons numerically, the following procedure has been used by Kozhokin, Kurizki and Malomed [1998]: Eqs. (4.26) were simulated for an initial configuration in the form of the ZV soliton multiplied by $\exp(ip\zeta)$ with some wavenumber p , in order to ‘push’ the soliton. The results demonstrate that, at sufficiently small p , the ‘push’ indeed produces a moving stable soliton (Fig. 7(a)). However, if p is large enough, the multiplication by $\exp(ip\zeta)$ turns out to be a more violent perturbation, splitting the initial pulse into two solitons, one quiescent and one moving (Fig. 7(b)).

Another one-parameter subfamily of moving GS was found in the exact form of a phase-modulated 2π -soliton by Kozhokin and Kurizki [1995]:

$$\Sigma_+ = A_0 \exp[i(\kappa\zeta - \chi\tau)] \operatorname{sech}[\beta(\zeta - v\tau)], \quad (5.18)$$

where χ is the detuning from the gap center, A_0 is the amplitude of the solitary pulse, β its width and v its group velocity.

Substituting $\partial_\tau P$ from Eq.(4.23a) into Eq.(4.21a), we may express P in terms of Σ_+ and the population inversion w . Then, upon eliminating P and using ansatz Eq.(5.18), we can integrate Eq.(4.23b) for the population inversion w , obtaining

$$w = -1 - \frac{A_0^2(\chi - \kappa/v)}{2(\delta - \eta)} \frac{1}{\cosh^2[\beta(\zeta - v\tau)]}. \quad (5.19)$$

Using these explicit expressions for P and w in Eqs.(4.21a) and (4.23a), we reduce our system to a set of algebraic equations for the coefficients κ , χ that determine

the spatial and temporal phase modulation, and the pulse width β as functions of the velocity v .

$$2(\chi - \kappa/v) - (1 - 1/v^2)(\delta - \eta) = 0, \quad (5.20a)$$

$$(\chi - \delta)(\beta^2 v^2 - \beta^2 + \kappa^2 - \chi^2 + \eta^2 + 2) + 2\beta^2 v^2(\chi - \kappa/v) + 2(\delta - \eta) = 0, \quad (5.20b)$$

$$(\beta^2 v^2 - \beta^2 + \kappa^2 - \chi^2 + \eta^2 + 2) - 2(\chi + \delta)(\chi - \kappa/v) = 0. \quad (5.20c)$$

The soliton amplitude is then found to satisfy $|A_0| = 2\beta v$, exactly as in the case of usual SIT (see Ch. 3). This implies, by means of Eq.(5.18), that the area under the Σ_+ envelope is 2π .

Let us consider the most illustrative case, when the atomic resonance is exactly at the center of the optical gap, $\delta = 0$. Then the solutions for the above parameters are

$$\kappa = -\frac{\eta}{2v} \frac{1 - 3v^2}{1 - v^2}, \quad (5.21a)$$

$$\chi = \frac{\eta}{2} \frac{1 + v^2}{1 - v^2}, \quad (5.21b)$$

$$\beta^2 v^2 = |A_0|^2/4 = \frac{8v^2(1 - v^2) - \eta^2(1 + v^2)^2}{4(1 - v^2)^2}. \quad (5.21c)$$

In the frame moving with the group velocity of the pulse, $\zeta' = \zeta - v\tau$, the temporal phase modulation will be $(\kappa v - \chi)\tau$, which is found from Eq.(5.21) to be equal to $-\eta\tau$. Since η is the (dimensionless) ‘bare’ gap width (see Ch. 4, this means that the frequency is detuned in the moving frame exactly to the band-gap edge. The band-gap edge corresponds (by definition) to a standing wave, whence this result demonstrates that such a pulse is indeed a soliton, which does not disperse in its group-velocity frame.

The allowed range of the solitary group velocities may be determined from Eq.(5.21c) through the condition $\beta^2 > 0$ for a given η . The same condition implies $|\eta| < \eta_{\max}$, where

$$\eta_{\max}^2 = \frac{8v^2(1 - v^2)}{(1 + v^2)^2}. \quad (5.22)$$

It follows from Eq.(5.22) that the condition for 2π SIT gap soliton (5.18) is $|\eta| < 1$, $\eta_{\max} = 1$ corresponding to $v = 1/\sqrt{3}$. This condition means that the cooperative *absorption length* $c\tau_0/n_0$ should be *shorter than the reflection (attenuation) length* in the gap $4c/(a_1\omega_c n_0)$, i.e., that the incident light should be absorbed by the TLS before it is reflected by the Bragg structure. In addition, both these lengths should be much longer than the light wavelength for the weak-reflection and slow-varying approximation to be valid.

From Eq.(4.21b) we find $\Sigma_- = \Sigma_+/v$. The envelopes of both waves (forward and backward) propagate in the same direction; therefore the group-velocity of the backward wave is in the direction opposite to its phase-velocity! This is analogous to climbing a descending escalator.

Analogously to Kerr-nonlinear gap solitons (Ch. 2), the real part of the non-linear polarization $\text{Re}P$ creates a traveling ‘defect’ in the periodic Bragg reflector

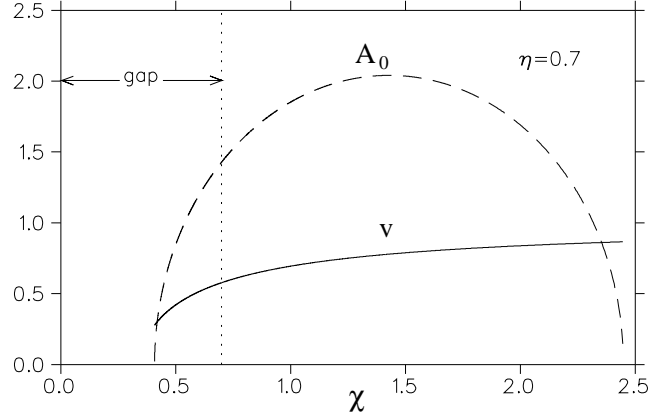


Figure 8: Dependence of the solitary pulse velocity (solid line) and amplitude (dashed line) in RABR on frequency detuning from the gap center for $\eta = 0.7$. The ‘bare’ gap edge marked by dotted line.

structure which allows the propagation at band-gap frequencies. The real part of the nonlinear polarization is governed by the frequency detuning from the TLS resonance. Exactly on resonance (which we here take to coincide with the gap center) $\chi = \delta = 0$, $\text{Re}P = 0$, and our solutions (5.21) yield imaginary values of the velocity v and modulation coefficient κ . The forward field envelope then decays with the same exponent as in the absence of TLS in the structure. Because of this mechanism, SIT exists only on one side of the band-gap center, depending on whether the TLS are in the region of the higher or the lower linear refractive index. This result may be understood as the addition of a near-resonant non-linear ‘refractive index’ to the modulated index of refraction of the gap structure. When this addition compensates the linear modulation, soliton propagation becomes possible (see Fig.3). On the ‘wrong’ side of the band-gap center, *soliton propagation is forbidden even in the allowed zone*, because the nonlinear polarization then cannot compensate even for a very weak loss of the forward field due to reflection.

The soliton amplitude and velocity dependence on frequency detuning from the gap center (which coincides with atomic resonance) are illustrated in Fig.8. They demonstrate that forward soliton propagation is allowed well within the gap, for χ satisfying $(1 - \sqrt{1 - \eta^2})/\eta < \chi < (1 + \sqrt{1 - \eta^2})/\eta$. In addition to frequency detuning from resonance, the near-resonant GS possesses another unique feature: spatial self-phase modulation $\kappa\zeta$ of both the forward and backward field components.

5.3. NUMERICAL SIMULATIONS

To check the stability of the analytical solution Eq.(5.18), as well as the possibility to launch a moving GS by the incident light field, numerical simulations of Eqs.(4.6) were performed by Kozhokin and Kurizki [1995]. As the launching condition, the incident wave was taken in the form $\mathcal{E}_F = A \exp[i\chi(t - t_0)] / \cosh[\beta(t - t_0)/\tau_0]$ without a backward wave ($\mathcal{E}_B = 0$) at the boundary of the sample $z = 0$. By varying the detuning χ and amplitude A we investigate the field evolution inside the

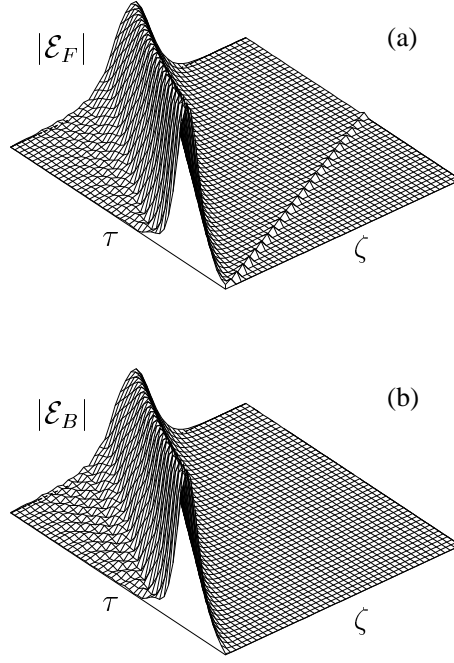


Figure 9: Numerical simulations of the intensities of (a) ‘forward’ and (b) ‘backward’ waves in the RABR gap, when Eqs.(5.21), (5.22) are obeyed ($\eta = 0.7$, group velocity $v \sim 0.3$)

structure. When these parameters are close to those allowed by Eqs.(5.21), (5.22), we observe the formation and lossless propagation of both forward and backward soliton-like pulses with amplitude ratios predicted by our solutions (Fig.9). By contrast, exponential decay of the forward pulse in the gap is numerically obtained in the absence of TLS (Fig.10).

The analysis surveyed in Secs. 5.1-5.3 strongly suggests, but does not rigorously prove, that the solution subfamily (5.18) belongs to a far more general two-parameter family, whose other particular representatives are the exact ZV solitons (5.11) and the approximate small-amplitude solitons determined by Eq. (5.17).

5.4. COLLISIONS BETWEEN GAP SOLITONS

An issue of obvious interest is that of collisions between GSs moving at different velocities in RABR. In the asymptotic small-amplitude limit reducing to the NLS equation (5.17), the collision must be elastic. To get a more general insight, we simulated collisions between two solitons given by (5.18). The conclusion is that the collision is *always inelastic*, directly attesting to the nonintegrability of the model. Typical results are displayed in Fig. 11, which demonstrates that the inelasticity may be strong, depending on the parameters.

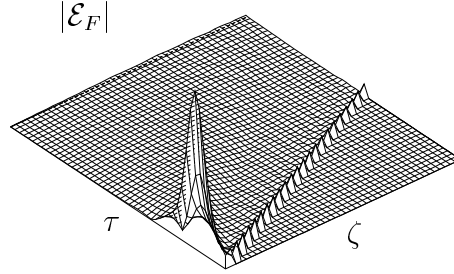


Figure 10: Numerical simulations of the intensities of ‘forward’ waves in the RABR gap without TLS (same η and incident pulse as in Fig.9).

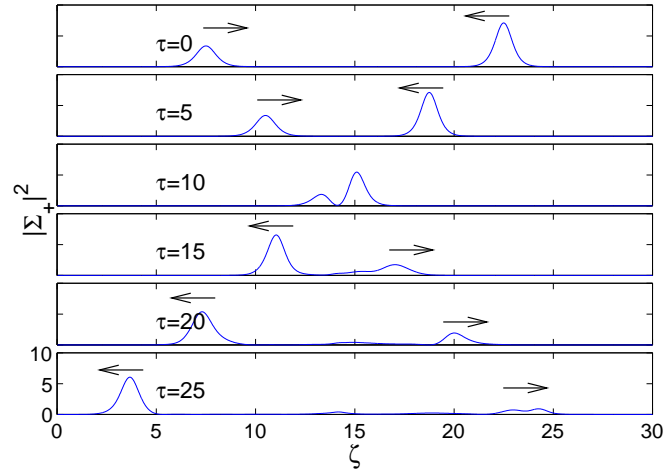


Figure 11: Typical example of inelastic collisions between the RABR solitons (5.18) at $\delta = 0$ and $\eta = 0.5$, with the velocities (normalized to c) $u_1 = 0.6$, $u_2 = -0.75$.

§ 6. Dark solitons in RABR

6.1. EXISTENCE CONDITIONS AND THE FORM OF THE SOLITON

Dark solitons (DSs) in RABR have been studied by Opatrný, Malomed and Kurizki [1999]. They are obtained similarly to the bright ones, by solving Eq. (5.4) with the potential (5.5). The potential will give rise to DS's provided that it has two symmetric maxima (see Fig. 5). In this case the quadratic part of the potential is convex, i.e., $|\chi| < \eta$, and the second (asymptotically linear) part of the expression (5.5) is concave, so that $\chi > \delta$. From these two inequalities, a simple necessary restriction on the model's parameters follows,

$$\delta < \eta. \quad (6.1)$$

The condition for the existence of the symmetric maxima determines the following frequency interval χ (recall that η is defined to be positive):

$$\max\{\delta, -\eta\} < \chi < \min\{\chi_2, \eta\}, \quad (6.2)$$

Making use of (5.8), one can easily check that, once the condition (6.1) is satisfied, the DS-supporting band (6.2) *always* exists. The DS frequency range defined by Eq. (6.2) is marked by shading (to the right from zero) in Fig. 4. The maxima of the potential are located at the points

$$\mathcal{S}_M = \pm \sqrt{4(\eta + \chi)^{-2} - (\chi - \delta)^2}, \quad (6.3)$$

which correspond to the polarization values

$$\mathcal{P}_M = \mp \sqrt{1 - (1/4)(\chi - \delta)^2(\chi + \eta)^2}. \quad (6.4)$$

Integrating Eq. (5.4) by means of energy conservation in the formal mechanical problem, we obtain $\mathcal{S}(\zeta)$ in an implicit form,

$$\begin{aligned} \zeta &= \pm \frac{1}{\sqrt{2}} \int_0^{\mathcal{S}} \frac{d\mathcal{S}_1}{\sqrt{U_M - U(\mathcal{S}_1)}} \\ &\equiv \pm \frac{1}{\sqrt{2}} \int_0^{\mathcal{S}} \frac{d\mathcal{S}_1}{\sqrt{U_M + \alpha\mathcal{S}_1^2 - \beta\sqrt{\gamma^2 + \mathcal{S}_1^2}}}, \end{aligned} \quad (6.5)$$

with

$$\alpha \equiv \frac{1}{2}(\eta^2 - \chi^2), \quad \beta \equiv 2(\eta - \chi), \quad \gamma \equiv \chi - \delta. \quad (6.6)$$

The solution (6.5) corresponds to a trajectory beginning at the potential maximum $\pm\mathcal{S}_M$ at 'time' $\zeta = -\infty$ and arriving at the other maximum, $\mp\mathcal{S}_M$ at 'time' $\zeta = \infty$ (see Fig. 5). In terms of the Σ_+ mode of the electric field, this is exactly a quiescent (zero-velocity) DS with the background cw amplitude \mathcal{S}_M .

The integral (6.5) can be formally expressed in terms of incomplete elliptic integrals, but, practically, it is more helpful to evaluate it numerically. As in Ch. 5, the polarization amplitude \mathcal{P} is determined by \mathcal{S} via Eq. (5.2) and the amplitude

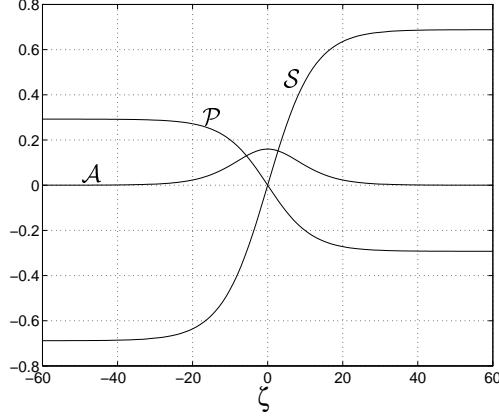


Figure 12: A typical example of a dark soliton, presented in terms of the variables S , P and \mathcal{A} . The parameters are $\eta = 0.6$, $\delta = -2$, and $\chi = 0.25$

of the Σ_- mode is obtained by solving Eq. (5.15). An example of the amplitude S for DS in the Σ_+ mode, together with the corresponding quantities P and \mathcal{A} , are plotted in Fig. 12.

The energy density of the $|\Sigma_+|^2$ field mode always has the shape of a hole in the background (see Fig. 13). The energy density of $|\Sigma_-|^2$ has a hump, which is the counterpart of the hole in the Σ_+ mode. The net electromagnetic energy density may have either a hole (which never drops to zero) or a hump, depending on the system parameters η , δ , and the soliton frequency χ .

6.2. THE BACKGROUND STABILITY

An obvious necessary condition for the stability of DS is the stability of its cw background. To tackle this problem, we use Eq. (4.26b) to eliminate Σ_+ in favor of P ,

$$\Sigma_+ = -(P_\tau - i\delta P)(1 - |P|^2)^{-1/2}, \quad (6.7)$$

and insert it into Eq. (4.26a). The resulting equation for P is linearized around the stationary value \mathcal{P}_M (see Eq. (6.4)), substituting

$$P = \mathcal{P}_M e^{-i\chi\tau} [1 + a(\zeta, \tau) + i b(\zeta, \tau)], \quad (6.8)$$

where a and b are small real perturbations. We can look for its general solution in the form (cf. Eq. (4.56c)),

$$a(\zeta, \tau) = a_0 e^{i(\kappa\zeta - \Omega\tau)}, \quad b(\zeta, \tau) = b_0 e^{i(\kappa\zeta - \Omega\tau)}, \quad (6.9)$$

which leads to a dispersion relation for Ω and κ , that consists of two parts:

$$\begin{aligned} & -(\chi - \delta)(\chi + \eta)^2 \Omega^3 - 2[\chi(\chi - \delta)(\chi + \eta)^2 + 2] \Omega^2 \\ & + [(\eta + \chi)^3(\eta - \delta)(\chi - \delta) - 8\chi + (\chi - \delta)(\chi + \eta)^2 \kappa^2] \Omega \\ & + (\eta^2 - \chi^2)[4 - (\chi - \delta)^2(\eta + \chi)^2] + 4\kappa^2 = 0, \end{aligned} \quad (6.10)$$

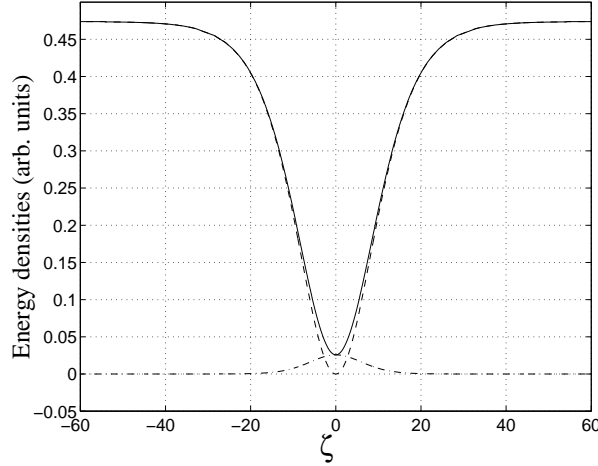


Figure 13: Field energy densities as a function of the coordinate ζ inside the dark soliton shown in Fig.12: $|\Sigma_+|^2$ (dashed line), $|\Sigma_-|^2$ (dash-dotted line), and their sum (continuous line).

and

$$-\Omega^3 - (3\chi - \delta)\Omega^2 + [(\eta - \chi)(2\chi + \eta - \delta) + \kappa^2]\Omega + (\chi - \delta)\kappa^2 = 0. \quad (6.11)$$

As checked numerically by Opatrný, Malomed and Kurizki [1999] for many values of η , δ and χ that support DS's according to the results obtained in the previous section, all the roots of (6.10) and (6.11) are real for *any* real κ . This implies the stability of the background for these values of η , δ and χ .

Equations (6.10) and (6.11) represent new dispersion relations, which are valid under the condition of strong background field \mathcal{S}_M and replace the zero-field dispersion relations of Eq. (4.57). This kind of optical bistability can be compared to the distributed feedback bistability with Kerr nonlinearity studied by Winful, Marburger and Garmire [1979].

6.3. DIRECT NUMERICAL STABILITY TESTS

Even though there is no evidence of background instability, it is necessary to simulate the full system of the partial differential equations, in order to directly test the DS stability. Equations (4.26a) and (4.26b) have been integrated numerically by Opatrný, Malomed and Kurizki [1999], with initial conditions differing from the exact DS solution by a small perturbation added to it. The results strongly depend on the parameters η , δ and χ : for some values, an explosion of the initial perturbation occurs, leading to a completely irregular pattern, whereas for others the DS shape remained *virtually undisturbed*. The dependence of the stability on the parameters η and χ with fixed δ is shown in Fig. 14. The darkest area of the DS parameter region corresponds to the stable regime where no instability has occurred during the entire simulation time (typically, $\tau \sim 500$). In the rest of the parameter region, DS's are unstable: in the lightest part of the DS region, the instability develops

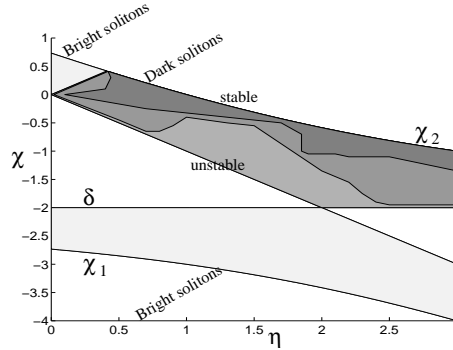


Figure 14: Parameter regions (η vs. χ) for dark (Eq. (6.2)) and bright (Eqs. (5.6) and (5.7)) solitons at $\delta = -2$. The boundaries χ_1 and χ_2 are given by Eq. (5.8). In the DS region, the darkest area corresponds to stable behavior whereas in the remaining part the (numerical) solutions are unstable: in the lightest area (of DS's) instability develops very quickly, while in the intermediate area the DS exists for a much longer time before the onset of the instability.

very quickly (at $\tau < 50$), whereas in the intermediate part, the instability builds up relatively slowly. As can be seen, the unstable behavior occurs closer to the boundaries of the existence region, $\chi = \pm \eta$ and $\chi = \delta$, whereas along the boundary $\chi = \chi_2$ (corresponding to the DS-supporting background which degenerates into the trivial zero solution), DS's are stable.

6.4. COEXISTENCE OF THE DARK AND BRIGHT SOLUTIONS

A very interesting question is whether the system can support bright and dark solitons at the *same values* of the parameters. As mentioned above, DS's always exist in the frequency interval (6.2), once the inequality (6.1) is satisfied. On the other hand, bright solitons are found in two frequency bands χ , given in Eqs. (5.6) and (5.7). From the discussion in Ch. 5 it follows that the DS frequency band *always coexists* with one or two bands supporting the bright solitons. The special case when there are *two* bright-soliton bands coexisting with the DS band is singled out by the condition

$$\eta - \frac{1}{\eta} < \delta < \eta. \quad (6.12)$$

One can readily check that the coexisting frequency bands supporting bright and dark solitons never overlap, i.e., quite naturally, the bright and dark solitons cannot have the same frequency.

6.5. MOVING DARK SOLITONS

Thus far we have considered only the quiescent DS's. A challenging question is whether they also have their moving counterparts. Adding the velocity parameter to the exact DS solution is not trivial, as the underlying equations (4.26a) and (4.26b) have no Galilean or Lorentzian invariance. The physical reason for this is

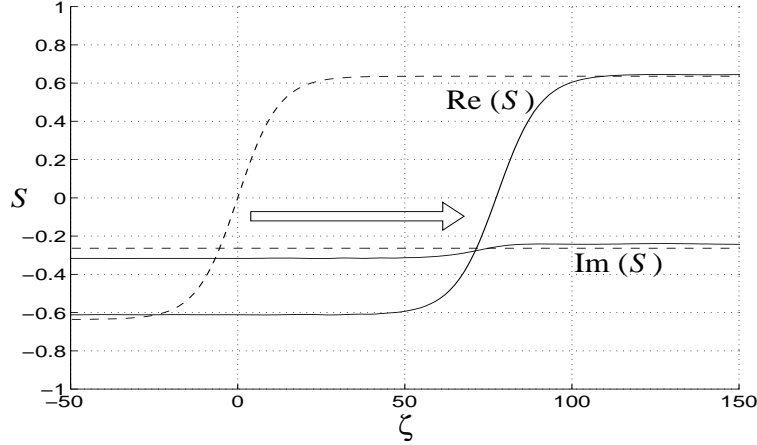


Figure 15: Moving dark soliton: the values of the parameters are the same as in Fig. 12, the background phase-jump parameter ϕ (see Eqs. (6.13) and (6.14)) is $\phi = -\pi/4$. Dashed line: $\tau = 0$, continuous line: $\tau = 600$.

the existence of the special (laboratory) reference frame, in which the Bragg grating is at rest.

In principle it is possible, in analogy to the stationary solutions and Eq. (5.1), substitute functions of the argument $(\zeta - v\tau)$ into the set (4.26a) and (4.26b) to obtain an ordinary differential equation. However, this would be a complicated complex nonlinear equation of the third order, containing all the lower-order derivatives, so that we would not be able to take advantage of the Newton-like structure, as in Ch. 5 and 6. Though it is possible to solve such an equation numerically, it is more suitable to deal with the original set of partial differential equations, in order to better understand the nature of the evolution.

In contrast to the case of bright solitons where the moving solutions can be found by multiplying, in the initial conditions, the quiescent DS by a factor proportional to $\exp(i\kappa\zeta)$ (see Kozhokin, Kurizki and Malomed [1998] and Ch. 5), it has proven possible to generate *stable moving* DS's from the quiescent ones in a different way (Opatrný, Malomed and Kurizki [1999]). To this end, recall that a DS corresponds to a transition between two different values of the background cw field. The background field takes, generally, complex values (note the real values in the expressions (6.3) and (6.4) are only our choices adopted above for convenience). The quiescent DS corresponds to a transition between two background values with phases differing by π . A principal difference of the DS's in the present model from those in the NLS equation (Kivshar and Luther-Davies [1998]) is that here a moving DS is generated by introducing a *phase jump* $\neq \pi$ across the DS.

Thus, one can take the initial condition for the system of equations (4.26a) and

(4.26b) as

$$\Sigma_+(\zeta, 0) = \cos\left(\frac{\phi}{2}\right) \mathcal{S}_q(\zeta) + i \sin\left(\frac{\phi}{2}\right) \mathcal{S}_M, \quad (6.13)$$

$$P = \cos\left(\frac{\phi}{2}\right) \mathcal{P}_q(\zeta) + i \sin\left(\frac{\phi}{2}\right) \mathcal{P}_M, \quad (6.14)$$

where \mathcal{S}_q and \mathcal{P}_q are the (real) functions corresponding to the quiescent DS, \mathcal{S}_M and \mathcal{P}_M are given by Eqs. (6.3), (6.4) and ϕ is the deviation from π of the background phase jump across DS. A typical result obtained by means of this modification of the initial state is displayed in Fig. 15: the DS moves at a velocity that is proportional to ϕ . The resulting form of the moving DS is slightly different from that of the quiescent soliton. The moving DS appears to be stable over the entire simulation time.

§ 7. Light bullets (spatiotemporal solitons)

A promising direction is the study of solitons in resonantly absorbing multi-dimensional (2D and 3D) media, in which the quasi-1D periodic structures can be realized as thin homogeneous layers set perpendicular to the direction of light propagation. In such media, *spatiotemporal* solitons, i.e., those localized in all dimensions, both transverse (spatial proper) and longitudinal (effectively, temporal), may exist. Spatiotemporal optical solitons or ‘light bullets’ (LBs) in various nonlinear media are surveyed in Ch. 1.

Here we are concerned with LBs in RABRs that consist of thin TLS layers embedded in a 2D- or 3D- periodic dielectric medium. We will follow a recent analysis by Blaauboer, Kurizki and Malomed [2000], which extends an earlier prediction of stable LBs in uniform 2D and 3D SIT media (Blaauboer, Malomed and Kurizki [2000]).

We start by considering a 2D SIT medium with a refractive index $n(z, x)$ periodically modulated in the propagation direction z , which represents the quasi-one-dimensional Bragg grating. Light propagation in the medium is described by the lossless Maxwell-Bloch equations (Newell and Moloney [1992]):

$$-i \frac{\partial^2 \mathcal{E}}{\partial x^2} + n^2 \frac{\partial \mathcal{E}}{\partial \tau} + \frac{\partial \mathcal{E}}{\partial \zeta} + i(1 - n^2) \mathcal{E} - P = 0, \quad (7.1a)$$

$$\frac{\partial P}{\partial \tau} - \mathcal{E}w = 0, \quad (7.1b)$$

$$\frac{\partial w}{\partial \tau} + \frac{1}{2}(\mathcal{E}^* P + P^* \mathcal{E}) = 0. \quad (7.1c)$$

Here (as in Sec. 4.1) \mathcal{E} and P are the slowly varying amplitudes of the electric field and medium’s polarization, w is the population inversion, ζ and x are longitudinal and transverse coordinates (measured in units of the resonant-absorption length), and τ is time (measured in units of the input pulse duration). The Fresnel number, which governs the transverse diffraction in the 2D and 3D propagation, was incorporated into x , and the detuning of the carrier frequency ω_0 from the central atomic-resonance frequency was absorbed into \mathcal{E} and P . To neglect the polarization dephasing and inversion decay, we assume pulse durations that are short on

the time scale of the relaxation processes. Equations (7.1) are then compatible with the local constraint $|P|^2 + w^2 = 1$, which represents the so-called Bloch-vector conservation. In a 1D case, i.e., in the absence of the x -dependence and for $n(z, x) = 1$, Eq. (7.1a) reduces to the sine-Gordon (SG) equation, which has a commonly known soliton solution, see Eq.(3.11) and Ch.3.

To search for LBs in a 2D medium subject to a resonant periodic longitudinal modulation, one may assume a periodic modulation of the refractive index as per Eq.(4.1). The RABR is then constructed by placing very thin layers (much thinner than $1/k_c$) of two-level atoms, whose resonance frequency is close to ω_c , at *maxima* of this modulated refractive index.

The objective is to consider the propagation of an electromagnetic wave with a frequency close to ω_c through a 2D RABR. Due to the Bragg reflections, the electric field \mathcal{E} gets decomposed into forward- and backward-propagating components \mathcal{E}_F and \mathcal{E}_B , which satisfy equations that are a straightforward generalization of the 1D equations derived by Kozhokin and Kurizki [1995], Kozhokin, Kurizki and Malomed [1998], and Opatrný, Malomed and Kurizki [1999] (see also Eqs. (4.21) and (4.23) in this review):

$$-i\frac{\partial^3\Sigma_+}{\partial\tau x^2} + i\frac{\partial^3\Sigma_-}{\partial\zeta x^2} + \frac{\partial^2\Sigma_+}{\partial\tau^2} - \frac{\partial^2\Sigma_+}{\partial\zeta^2} \quad (7.2a)$$

$$+ \eta\frac{\partial^2\Sigma_+}{\partial x^2} + \eta^2\Sigma_+ - 2\frac{\partial P}{\partial\tau} - 2i\eta P = 0,$$

$$-i\frac{\partial^3\Sigma_-}{\partial\tau x^2} + i\frac{\partial^3\Sigma_+}{\partial\zeta x^2} + \frac{\partial^2\Sigma_-}{\partial\tau^2} - \frac{\partial^2\Sigma_-}{\partial\zeta^2} \quad (7.2b)$$

$$- \eta\frac{\partial^2\Sigma_-}{\partial x^2} + \eta^2\Sigma_- + 2\frac{\partial P}{\partial\zeta} = 0,$$

$$\frac{\partial P}{\partial\tau} + i\delta P - \Sigma_+ w = 0, \quad (7.2c)$$

$$\frac{\partial w}{\partial\tau} + \frac{1}{2}(\Sigma_-^* P + \Sigma_+ P^*) = 0. \quad (7.2d)$$

Here Σ_{\pm} is defined by Eq. (4.9), and η is a ratio of the resonant-absorption length in the two-level medium to the Bragg-reflection length, which was defined above by Eq. (4.13).

To construct an analytical approximation to the LB solutions, the starting point adopted by Blaauboer, Kurizki and Malomed [2000] is a subfamily of the exact 1D soliton solutions to Eqs. (7.2), which was found by Kozhokin and Kurizki [1995] (see also Sec. 5.2 in this review) and is given by Eqs.(5.18) and (5.19). These solutions were taken with parameters satisfying Eqs.(5.20):

$$A_0 = 2\sqrt{\frac{\delta}{\eta} - 1}, \quad \beta = \sqrt{\frac{\delta}{\eta} + 1}, \quad v = -\sqrt{\frac{\delta - \eta}{\delta + \eta}}, \quad (7.3a)$$

$$\kappa = -\sqrt{\delta^2 - \eta^2}, \quad \text{and} \quad \chi = \delta. \quad (7.3b)$$

These solutions were chosen as a pattern to construct an approximate solution for LBs because the shape of the fields Σ_+ and Σ_- in the solutions is similar to that of the SG soliton in the 1D uniform SIT medium (see Sec. 3.1). Inspired by this

analogy and by the fact that there exist LBs in the uniform 2D SIT medium which reduce to the SG solitons in the 1D limit (Blaauboer, Malomed and Kurizki [2000]), one can search for an approximate LB solution to the 2D equations (7.2), which also reduces to the exact soliton in 1D. To this end, the following approximation was assumed:

$$\Sigma_+ = A_0 \sqrt{\operatorname{sech}\Theta_1 \operatorname{sech}\Theta_2} e^{i(\kappa\zeta - \chi\tau) + i\pi/4}, \quad (7.4a)$$

$$\Sigma_- = \Sigma_+ / v, \quad (7.4b)$$

$$P = \sqrt{\operatorname{sech}\Theta_1 \operatorname{sech}\Theta_2} \left\{ (\tanh\Theta_1 + \tanh\Theta_2)^2 + \frac{\delta - \eta}{4\eta} C^4 [(\tanh\Theta_1 - \tanh\Theta_2)^2 - 2(\operatorname{sech}^2\Theta_1 + \operatorname{sech}^2\Theta_2)]^2 \right\}^{1/2} e^{i(\kappa\zeta - \chi\tau) + i\nu}, \quad (7.4c)$$

$$w = [1 - |P|^2]^{1/2}, \quad (7.4d)$$

with $\Theta_1(\tau, \zeta) \equiv \beta(\zeta - v\tau) + \Theta_0 + Cx$, $\Theta_2(\tau, \zeta) \equiv \beta(\zeta - v\tau) + \Theta_0 - Cx$, the phase ν and coefficients Θ_0 and C being real constants, while the other parameters are defined by Eqs.(7.3).

The ansatz (7.4) satisfies Eqs. (7.2a) and (7.2b) exactly, while Eqs. (7.2d) are satisfied to order $\sqrt{\delta/\eta - 1}C^2$, which requires that $\sqrt{\delta/\eta - 1}C^2 \ll 1$. The ansatz applies for *arbitrary* η , admitting *both* weak ($\eta \ll 1$) and strong ($\eta > 1$) reflectivities of the Bragg grating, provided that the detuning remains small with respect to the gap frequency. Comparison with numerical simulations of Eqs. (7.2), using Eq. (7.4) as an initial configuration (a finite-difference method, with Fourier transform scheme, described by Drummond [1983], was used), tests this analytical approximation and shows that it is indeed fairly close to a numerically exact solution; in particular, the shape of the bullet remains within 98% of its originally presumed shape after having propagated a large distance, as is shown in Fig. 16.

Three-dimensional LB solutions with axial symmetry have also been constructed in an approximate analytical form and successfully tested in direct simulations, following a similar approach (Blaauboer, Kurizki and Malomed [2000]). Generally, they are not drastically different from their 2D counterparts described above.

A challenging problem which remains to be considered is the construction of *spinning* light bullets in the 3D case (doughnut-shaped solitons, with a hole in the center, carrying an intrinsic angular momentum). Recently, spinning bullets were found by means of a sophisticated version of the variational approximation in a simpler 3D model, viz., the nonlinear Schrödinger equation with self-focusing cubic and self-defocusing quintic nonlinearities, by Desyatnikov, Maimistov and Malomed [2000]. Further direct simulations have demonstrated that these spinning bullets (unlike their zero-spin counterparts) are always subject to an azimuthal instability, that eventually splits them into a few moving zero-spin solitons, although the instability can sometimes be very weak (Mihalache, Mazilu, Crasovan, Malomed and Lederer [2000]). At present, it is not known whether spinning LBs can be completely stable in any 3D model.

It is relevant to stress that two- (and three-) dimensional LB solutions of the variable-separated form, $\Sigma_{\pm} \sim \Sigma_{\pm} \sim f(\tau, \zeta) \cdot g(x)$, do *not* exist in the RABR model. Indeed, the substitution of this into Eqs. (7.2a) and (7.2b) yields only a plane-wave solution of the form $\Sigma_{\pm} \sim \exp(iA\tau + iBx)$, with constant A and B .

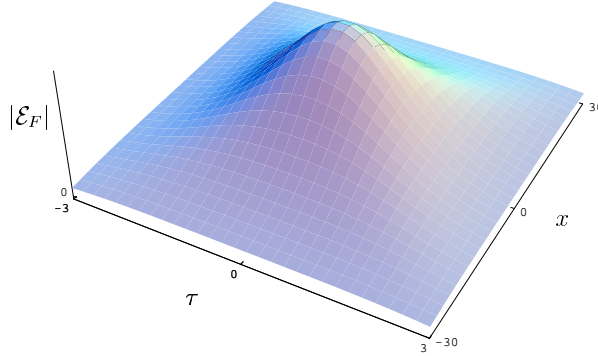


Figure 16: The forward-propagating electric field of the two-dimensional ‘light bullet’ in the Bragg reflector, $|\mathcal{E}_F|$, vs. time τ and transverse coordinate x , after having propagated the distance $z = 1000$. The parameters are $\eta = 0.1$, $\delta = 0.2$, $C = 0.1$ and $\Theta_0 = -1000$. The field is scaled by the constant $\hbar/4\tau_0\mu n_0$.

§ 8. Experimental prospects and conclusions

This review has focused on properties of solitons in RABR, combining a periodic refractive-index (Bragg) grating and a periodic set of thin active layers (consisting of two-level systems *resonantly* interacting with the field). It has been demonstrated that the RABR supports a vast family of bright gap solitons, whose properties differ substantially from their counterparts in periodic structures with either cubic or quadratic *off-resonant* nonlinearities reviewed in Ch. 2.

The same RABR can support, depending on the initial conditions, either dark or bright stable solitons, without any changes of the system parameters, which is a unique feature for nonlinear optical media (Ch. 5, 6). Zero-velocity dark solitons can be found in an analytical form, as well as traveling dark solitons with a constant phase difference ($\neq \pi$) of the background amplitudes across the soliton (Ch. 6). The latter property is a major difference with respect to dark solitons of the NLS equation, whose motion is supported by giving the background a nonzero wavenumber.

Depending on the values of the parameters, the frequency band of the quiescent dark solitons coexists with one or two bands of the stable bright ones, without an overlap. Direct numerical simulations demonstrate that some dark-soliton solutions are stable against arbitrary small perturbations, whereas others are unstable when they are close to the “dangerous” boundaries of their existence domain.

A multidimensional version of the RABR model, corresponding to a periodic set of thin active layers placed at the maxima of the refractive index, which is modulated along the propagation direction of light has been considered too. It has been found to support stable propagation of spatiotemporal solitons in the form of two- and three-dimensional ‘light bullets’ (LBs).

The best prospect of realizing a RABR which is adequate for observing the solitons and light bullets discussed in Ch. 5 - Ch. 7 is to use thin layers of *rare-earth*

ions (Greiner, Boggs, Loftus, Wang and Mossberg [1999]) embedded in a spatially-periodic semiconductor structure (Khitrova, Gibbs, Jahnke, Kira and Koch [1999]). The two-level atoms in the layers should be rare-earth-ions with the density of $10^{15} - 10^{16} \text{ cm}^{-3}$, and large transition dipole moments. The parameter η can vary from 0 to 100 and the detuning is $\sim 10^{12} - 10^{13} \text{ s}^{-1}$.

Cryogenic conditions in such structures can strongly extend the dephasing time T_2 and thus the soliton's or LB's lifetime, well into the μsec range (Greiner, Boggs, Loftus, Wang and Mossberg [1999]), which would greatly facilitate the experiment. The construction of suitable structures constitutes a feasible experimental challenge.

In a RABR with the transverse size of $10 \mu\text{m}$, LBs can be envisaged to be localized on the time and transverse-length scales, respectively, $\sim 10^{-12} \text{ s}$ and $1 \mu\text{m}$. The incident pulse has uniform transverse intensity and the transverse diffraction is strong enough. One needs $d^2/l_{\text{abs}}\lambda_0 < 1$, where l_{abs} , λ_0 and d are the resonant-absorption length, carrier wavelength, and the pulse diameter, respectively (Slusher [1974]). For $l_{\text{abs}} \sim 10^{-3} \text{ m}$ and $\lambda_0 \sim 10^{-4} \text{ m}$, one thus requires $d < 10^{-4} \text{ m}$, which implies that the transverse medium size L_x must be a few μm .

Effects of TLS dephasing and deexcitation in RABRs can be studied by substituting the values $-i\delta - \Gamma_2\tau_0$ for the frequency term $-i\delta$ in Eqs. (4.47) – (4.49) and the loss terms $-\Gamma_1\tau_0(w_0 + 1)$ in Eq. (4.50), $-\Gamma_1w_1$ in Eq. (4.51) and $-\Gamma_1(w_2 - 2)$ in Eq. (4.52). We have checked that these modifications *do not* influence the qualitative behavior of the solutions on the time scale $\tau\tau_0 < 1/\Gamma_{1,2}$.

Let us now discuss the experimental conditions for the realization of RABR solitons using *quantum wells* embedded in a semiconductor structure with periodically alternating linear index of refraction (Khitrova, Gibbs, Jahnke, Kira and Koch [1999]). We can assume the following values: the average refraction index is $n_0 \approx 3.6$, the wavelength (in the medium) $\lambda \approx 232 \text{ nm}$, which corresponds to the angular frequency $\omega_c \approx 2.26 \times 10^{15} \text{ s}^{-1}$. Excitons in quantum wells can, under certain conditions (such as low densities and proximity of the operating frequency to an excitonic resonance, see Khitrova, Gibbs, Jahnke, Kira and Koch [1999]) may be regarded as effective two-level systems (TLS's). We consider their surface density to be $\approx 10^{10} - 10^{11} \text{ cm}^{-2}$, which corresponds to a bulk density $\rho_0 \approx 10^{15} - 10^{16} \text{ cm}^{-3}$. If we assume that the excitons are formed by electrons and holes displaced by $\approx 1 - 10 \text{ nm}$, then the characteristic absorption time τ_0 defined in Eq. (3.8) is $\tau_0 \approx 10^{-13} - 10^{-12} \text{ s}$, and the corresponding absorption length is $c\tau_0/n_0 \approx 10 - 100 \mu\text{m}$. The *dephasing time* for excitons discussed by Khitrova, Gibbs, Jahnke, Kira and Koch [1999] is $1/\Gamma_2 \approx 10^{-13} \text{ s}$, which seems to be the *chief limitation* of the soliton lifetime for this system. The structures shown in Figs. 6, 12, 13, and 15, occupying regions of approximately 100 absorption lengths would require a device of the total width of approximately 1 mm to 1 cm, which corresponds to $\approx 10^3$ to 10^4 unit cells. The modulation of the refraction index can be as high as $a_1 \approx 0.3$, so that the parameter η (see Eq. (4.13)) can vary from 0 to 100. The unit of the dimensionless detuning δ would represent a $10^{-3} - 10^{-2}$ fraction of the carrier frequency. The intensities of the applied laser field corresponding to $\Sigma_{\pm} \approx 1$ are then of the order $10^6 - 10^7 \text{ W/cm}^2$.

In the work by Khitrova, Gibbs, Jahnke, Kira and Koch [1999], the width of the active layers (quantum wells) is considered to be $5 - 20 \text{ nm}$, which corresponds to the parameter γ^2 (see Eq. (4.29)) in the range $10^{-3} - 2 \times 10^{-2}$. In the simulations discussed by Opatrný, Malomed and Kurizki [1999], taking the largest of these

values and the parameters as in Fig. 12, i.e., $\eta = 0.6$, $\delta = -2$, and $\chi = 0.25$, we have observed the time evolution of the system (4.36a) – (4.52). As the initial condition, both the DS solution corresponding to zero width of the active layers and the DS solution including the finite width correction, have been taken. In both cases, the evolution was quite regular over the observed time $\tau \approx 50$, and the zero-width solution (with the quantities \mathcal{S} , \mathcal{P} , \mathcal{A} as given by Eqs. (6.5), (5.2) and (5.15)) started to change after $\tau \approx 10$.

We can now sum up the discussion of experimental perspectives for the realization of RABR solitons: *a*) The prospects appear to be good for gratings incorporating thin layers of rare-earth ions under cryogenic conditions. *b*) The realization of these solitons in excitonic superlattices would require much longer dephasing times than those currently achievable in such structures.

§ Acknowledgments

We are grateful to M. Blaauboer for discussions and help. G.K. acknowledges the support of ISF, Minerva and US-Israel BSF. T.O. thanks the Deutsche Forschungsgemeinschaft for support. A.K. acknowledges support of the Thomas B. Thriges Center for Quantum Information.

§ References

- Aceves, A. B., and S. Wabnitz, 1989, Self-induced transparency solitons in nonlinear refractive periodic media, *Phys.Lett. A* **141**, 37.
- Afanas'ev, A. A., V. M. Volkov, V. V. Dritz and B. A. Samson, 1990, Interaction of counter-propagating self-induced transparency solitons, *Journal of Modern Optics* **37** (2), 165–170.
- Agrawal, G. P., 1995, *Nonlinear Fiber Optics*, (Academic Press, San Diego).
- Aközbek, N., and S. John, 1998, Self-induced transparency solitary waves in a doped nonlinear photonic band gap material, *Phys. Rev. E* **58** (3), 3876 – 3895.
- Barashenkov, I. V., D. M. Pelinovsky and E. V. Zemlyanaya, 1998, Vibrations and oscillatory instabilities of gap solitons, *Phys. Rev. Lett.* **80** (23), 5117 – 5120.
- Basharov, A. M., 1988, Thin film of two-level atoms: a simple model of optical bistability and self-pulsation, *Sov.Phys. JETP* **67** (9), 1741–1744.
- Benedict, M. G., V. A. Malyshev, E. D. Trifonov and A. I. Zaitsev, 1991, Reflection and transmission of ultrashort light pulses through a thin resonant medium: Local-field effects, *Phys.Rev. A* **43** (7), 3845–3853.
- Blaauboer, M., G. Kurizki and B. A. Malomed, 2000, Spatiotemporally localized solitons in resonantly-absorbing Bragg reflectors, *Phys. Rev. E* **62** (1), (in press), e-print nlin.PS/0007004.
- Blaauboer, M., B. A. Malomed and G. Kurizki, 2000, Spatiotemporally localized multidimensional solitons in self-induced transparency media, *Phys. Rev. Lett.* **84** (9), 1906 – 1909.
- Bowden, C. M., A. Postan and R. Inguva, 1991, Invariant pulse propagation and self-phase modulation in dense media, *J. Opt. Soc. Am. B* **8** (5), 1081 – 1084.
- Brown, T. G., and B. J. Eggleton (Eds.), 1998, *Optics Express* **3** (11), Focus Issue: Bragg Solitons and Nonlinear Optics of Periodic Structures.

- Carter, S. J., P. D. Drummond, M. D. Reid and R. M. Shelby, 1987, Squeezing of quantum solitons, *Phys.Rev.Lett.* **58**, 1841 – 1844.
- Champneys, A. R., and B. A. Malomed, 2000, Embedded solitons in a three-wave system, *Phys. Rev. E* **61**, 886–890.
- Champneys, A. R., B. A. Malomed and M. J. Friedman, 1998, Thirring solitons in the presence of dispersion, *Phys. Rev. Lett.* **80**, 4169.
- Chen, Y. J., and J. Atai, 1995, Dark optical bullets in light self-trapping, *Opt. Lett.* **20**, 133–135.
- Cheng, Z., 1991, Pairing effect of photons in nonlinear polar crystals, *Phys. Rev. Lett.* **67** (20), 2788 – 2791.
- Cheng, Z., and G. Kurizki, 1995, Optical “multi-excitons”: Quantum gap solitons in nonlinear Bragg reflectors, *Phys. Rev. Lett.* **75**, 3430 – 3433.
- Chiao, R. Y., I. H. Deutsch, J. Garrison and E. W. Wright, 1993, Solitons in quantum nonlinear optics, In: Walther, H., N. Koroteev and M. O. Scully (Eds.), *Frontiers in Nonlinear Optics: The Serge Akhmanov Memorial Volume*, (IOP, Philadelphia), pp. 151 – 182.
- Christodoulides, D. N., and R. I. Joseph, 1989, Slow Bragg solitons in nonlinear periodic structures, *Phys. Rev. Lett.* **62**, 1746.
- Conti, C., S. Trillo and G. Assanto, 1997, Doubly resonant Bragg simultons via second-harmonic generation, *Phys. Rev. Lett.* **78** (12), 2341 – 2344.
- Crenshaw, M. E., and C. M. Bowden, 1992, Quasi-adiabatic following approximation for a dense medium of 2-level atoms, *Phys. Rev. Lett.* **69**, 3475.
- Crenshaw, M. E., M. Scalora and C. M. Bowden, 1992, Ultrafast intrinsic optical switching in a dense medium of 2-level atoms, *Phys. Rev. Lett.* **68**, 911.
- de Rossi, A., C. Conti and S. Trillo, 1998, Stability, multistability, and wobbling of optical gap solitons, *Phys. Rev. Lett.* **81** (1), 85–88.
- de Sterke, C. M., and J. E. Sipe, 1994, Gap solitons, In: Wolf, E. (Ed.), *Progress in Optics*, Vol. XXXIII, (Elsevier, North-Holland), Ch. 3, pp. 205 – 259.
- Desyatnikov, A., A. Maimistov and B. Malomed, 2000, Three-dimensional spinning solitons in dispersive media with the cubic-quintic nonlinearity, *Phys. Rev. E* **61** (3), 3107–3113.
- Deutsch, I. H., R. Y. Chiao and J. C. Garrison, 1992, Diphotons in a nonlinear Fabry-Perot resonator: Bound states of interacting photons in an optical “quantum wire”, *Phys.Rev.Lett.* **69**, 3627 – 3630.
- Deutsch, I. H., R. Y. Chiao and J.C.Garrison, 1993, Two-photon bound states: The diphoton bullet in dispersive self-focusing media, *Phys.Rev.A* **47**, 3330 – 3336.
- Dowling, J. P., and H. O. Everitt, 2000, Photonic & sonic band-gap bibliography. URL <http://home.earthlink.net/~jpdowling/pbgbib.html>
- Drummond, P. D., 1983, Central partial difference propagation algorithms, *Comp. Phys. Comm.* **29**, 211–225.
- Drummond, P. D., 1984, Formation and stability of vee simultons, *Opt. Comm.* **49**, 219–223.
- Drummond, P. D., S. J. Carter and R. M. Shelby, 1989, Time dependence of quantum fluctuations in solitons, *Optics Letters* **14** (7), 373 – 375.
- Drummond, P. D., and H. He, 1997, Optical mesons, *Phys. Rev. A* **56** (2), R1107–R1109.
- Drummond, P. D., R. M. Shelby, S. R. Friberg and Y. Yamamoto, 1993, Quantum solitons in optical fibers, *Nature* **365** (23), 307 – 313.

- Eggleton, B. J., R. E. Slusher, C. M. de Sterke, P. A. Krug and J. E. Sipe, 1996, Bragg grating solitons, *Phys. Rev. Lett.* **76** (10), 1627 – 1630.
- Etrich, C., F. Lederer, B. A. Malomed, T. Peschel and U. Peschel, 2000, Optical solitons in media with a quadratic nonlinearity, In: Wolf, E. (Ed.), *Progress in Optics*, (Elsevier, Amsterdam), in press.
- Feng, J., and F. K. Kneubuhl, 1993, Solitons in a periodic structure with Kerr nonlinearity, *IEEE Journal of Quantum Electronics* **29**, 590.
- Frantzeskakis, D., K. Hizanidis, B. Malomed and C. Polymilis, 1998, Stable anti-dark light bullets supported by the third-order dispersion, *Phys. Lett. A* **248** (2-4), 203–207.
- Greiner, C., B. Boggs, T. Loftus, T. Wang and T. W. Mossberg, 1999, Polarization-dependent rabi frequency beats in the coherent response of tm^{3+} in yag, *Phys. Rev. A* **60**, R2657–R2660.
- Haus, H. A., and Y. Lai, 1990, Quantum theory of soliton squeezing: a linearized approach, *JOSA B* **7**, 386 – 392.
- Hayata, K., and M. Koshiba, 1993, Multidimensional solitons in quadratic nonlinear media, *Phys. Rev. Lett.* **71**, 3275–3278.
- He, H., and P. D. Drummond, 1997, Ideal soliton environment using parametric band gaps, *Phys. Rev. Lett.* **78**, 4311–4315.
- He, H., and P. D. Drummond, 1998, Theory of multidimensional parametric band-gap solitons, *Phys. Rev. E* **58**, 5025–5046.
- Inguva, R., and C. M. Bowden, 1990, Spatial and temporal evolution of the first order phase transition in intrinsic optical bistability, *Phys. Rev. A* **41**, 1670.
- John, S., and T. Quang, 1995, Photon-hopping conduction and collectively induced transparency in a photonic band gap, *Phys. Rev. A* **52**, 4083–4088.
- John, S., and V. I. Rupasov, 1999, Quantum self-induced transparency in frequency gap media, *Europhysics Lett.* **46** (3), 326–331.
- Kanashov, A., and A. Rubenchik, 1981, *Physica D* **4**, 122.
- Kärtner, F. X., and H. A. Haus, 1993, Quantum-mechanical stability of solitons and the correspondence principle, *Phys. Rev. A* **48**, 2361 – 2369.
- Kheruntsyan, K. V., and P. D. Drummond, 1998a, Multidimensional parametric quantum solitons, *Phys. Rev. A* **58**, R2676–R2679.
- Kheruntsyan, K. V., and P. D. Drummond, 1998b, Three-dimensional quantum solitons with parametric coupling, *Phys. Rev. A* **58**, 2488–2499.
- Kheruntsyan, K. V., and P. D. Drummond, 2000, Multidimensional quantum solitons with nondegenerate parametric interactions: Photonic and Bose-Einstein condensate environments, *Phys. Rev. A* **61**, 063816.
- Khitrova, G., H. M. Gibbs, F. Jahnke, M. Kira and S. W. Koch, 1999, Nonlinear optics of normal-mode-coupling semiconductor microcavities, *Rev. Mod. Phys.* **71**, 1591–1640.
- Kivshar, Y., and B. Luther-Davies, 1998, Dark optical solitons: physics and applications, *Phys. Rep.* **298** (2-3), 81–197.
- Kozhokin, A., and G. Kurizki, 1995, Self-induced transparency in Bragg reflectors: Gap solitons near absorption resonances., *Phys. Rev. Lett.* **74** (25), 5020–5023.
- Kozhokin, A. E., G. Kurizki and B. Malomed, 1998, Standing and moving gap solitons in resonantly absorbing gratings, *Phys. Rev. Lett.* **81** (17), 3647.
- Kurizki, G., A. Kofman, A. Kozhokin and Z. Cheng, 1996, Cooperative and coherent optical processes in field confining structures, In: Rarity, J., and C. Weiss-

- buch (Eds.), *Microcavities and Photonic Bandgaps: Physics and Applications*, (Kluwer, London), pp. 559 – 572.
- Lai, Y., and H. A. Haus, 1989a, Quantum theory of solitons in optical fibers. I. Time-dependent Hartree approximation, *Phys.Rev.A* **40**, 844 – 853.
- Lai, Y., and H. A. Haus, 1989b, Quantum theory of solitons in optical fibers. II. Exact solution, *Phys.Rev.A* **40**, 854 – 866.
- Lakoba, T. I., 1994, Coherent pulse propagation in a discrete non-Bragg resonant medium, *Physics Letters A* **196**, 55.
- Lakoba, T. I., and B. I. Mantsyzov, 1992, Coherent interaction between a light pulse and the nonlinear inhomogeneous Bragg lattice, *Bulletin of the Russian Academy of Science Ph.* **56**, 1205.
- Lamb-Jr., G. L., 1971, Analytical description of ultrashort optical pulse propagation in resonant medium, *Rev.Mod.Phys* **43**, 99–124.
- Liu, X., L. J. Qian and F. W. Wise, 1999, Generation of optical spatiotemporal solitons, *Phys. Rev. Lett.* **82**, 4631–4634.
- Logvin, I. V. B. Y. A., and N. A. Loïko, 2000, Interrelation of spatial and temporal instabilities in a system of two nonlinear thin films, *Sov. Phys. JETP* **90**, 133–143.
- Logvin, Y. A., and A. M. Samson, 1992, Passage of light through a system of two bistable thin films, *Sov. Phys. JETP* **75** (2), 250 – 255.
- Maimistov, A., A. Basharov and S. Elyutin, 1990, Present state of self-induced transparency theory, *Phys.Rep.* **191**, 2.
- Mak, W. C. K., B. A. Malomed and P. L. Chu, 1998a, Solitary waves in coupled nonlinear waveguides with Bragg gratings, *J. Opt. Soc. Am. B* **15** (6), 1685–1692.
- Mak, W. C. K., B. A. Malomed and P. L. Chu, 1998b, Three-wave gap solitons in waveguides with quadratic nonlinearity, *Phys. Rev. E* **58**, 6708–6722.
- Malomed, B. A., P. Drummond, H. He, A. Berntson, D. Anderson and M. Lisak, 1997, Spatiotemporal solitons in multidimensional optical media with a quadratic nonlinearity, *Phys. Rev. E* **56**, 4725–4735.
- Malomed, B. A., and R. S. Tasgal, 1994, Vibration modes of a gap soliton in a nonlinear optical medium, *Phys. Rev. E* **49**, 5787.
- Mantsyzov, B. I., 1992, Solitons in periodic resonance media, *Bulletin of the Russian Academy of Science Ph.* **56**, 1284.
- Mantsyzov, B. I., 1995, Gap 2π pulse with an inhomogeneously broadened line and an oscillating solitary wave, *Phys. Rev. A* **51** (6), 4939–4943.
- Mantsyzov, B. I., and R. N. Kuz'min, 1984, Self-induced suppression of Bragg scattering of a resonant radiation pulse in a periodic medium, *Sov. Tech. Phys. Lett* **10** (7), 359–361.
- Mantsyzov, B. I., and R. N. Kuz'min, 1986, Coherent interaction of light with a discrete periodic medium, *Sov. Phys. JETP* **64**, 37.
- McCall, S. L., and E. L. Hahn, 1969, Self-induced transparency, *Phys.Rev* **183**, 457.
- McCall, S. L., and E. L. Hahn, 1970, Pulse-area-pulse-energy description of a travelling-wave laser amplifier, *Phys.Rev.A* **2**, 861.
- Mihalache, D., D. Mazilu, L.-C. Crasovan, B. Malomed and F. Lederer, 2000, Azimuthal instability of three-dimensional spinning solitons in cubic-quintic nonlinear media, *Phys. Rev. E* (in press).

- Mihalache, D., D. Mazilu, B. Malomed and L. Torner, 1998, Asymmetric spatio-temporal optical solitons in media with quadratic nonlinearity, *Opt. Comm.* **152** (4-6), 365–370.
- Newell, A. C., and J. V. Moloney, 1992, *Nonlinear Optics*, (Addison-Wesley, Redwood City CA).
- Opatrný, T., B. A. Malomed and G. Kurizki, 1999, Dark and bright solitons in resonantly absorbing gratings, *Phys. Rev. E* **60** (5), 6137 – 6149.
- Peschel, T., U. Peschel, F. Lederer and B. A. Malomed, 1997, Solitary waves in Bragg gratings with a quadratic nonlinearity, *Phys. Rev. E* **55** (4), 4730 – 4739.
- Poluektov, I. A., Y. M. Popov and V. S. Roitberg, 1975, Self-induced transparency, *Sov.Phys.-Usp.* **17**, 673.
- Rosenbluh, M., and R. M. Shelby, 1991, Squeezed optical solitons, *Phys.Rev.Lett.* **66**, 153.
- Rupasov, V. I., and M. Singh, 1996a, Quantum gap solitons and many-polariton-atom bound states in dispersive medium and photonic band gap, *Phys. Rev. Lett.* **77** (2), 338 – 341.
- Rupasov, V. I., and M. Singh, 1996b, Quantum gap solitons and soliton pinning in dispersive medium and photonic-band-gap materials: Bethe-ansatz solution, *Phys. Rev. A* **54** (4), 3614 – 3625.
- Rupasov, V. I., and V. I. Yudson, 1982, On boundary problems in the nonlinear optics of resonant media, *Sov. J. Quantum Electron.* **12**, 415.
- Rupasov, V. I., and V. I. Yudson, 1987, Nonlinear resonant optics of thin films: the inverse method, *Sov.Phys. JETP* **66**, 282.
- Scalora, M., and C. M. Bowden, 1995, Propagation effects and ultrafast optical switching in dense media, *Phys. Rev. A* **51** (5), 4048–4055.
- Scalora, M., J. P. Dowling, C. M. Bowden and M. J. Bloemer, 1994a, Optical limiting and switching of ultrashort pulses in nonlinear photonic band gap materials, *Phys. Rev. Lett* **73** (10), 1368–1371.
- Scalora, M., J. P. Dowling, C. M. Bowden and M. J. Bloemer, 1994b, The photonic band edge optical diode, *J. Appl. Phys.* **76** (4), 2023–2026.
- Schöllmann, J., and A. P. Mayer, 2000, Stability analysis for extended models of gap solitary waves, *Phys. Rev. E* **61** (5).
- Shaw, M. I., and B. W. Shore, 1990, Coherent atomic excitation in a cavity: I. Low density, *Journal of Modern Optics* **37** (5), 937–963.
- Shaw, M. I., and B. W. Shore, 1991, Collisions of counterpropagating optical solitons, *JOSA B* **8**, 1127.
- Silberberg, Y., 1990, Collapse of optical pulses, *Optics Letters* **15**, 1282–1285.
- Sizmann, A., and G. Leuchs, 1999, The optical Kerr effect and quantum optics in fibers, In: Wolf, E. (Ed.), *Progress in Optics*, Vol. XXXIX, (North-Holland, Amsterdam), Ch. V, pp. 373 – 469.
- Slusher, R. E., 1974, In: Wolf, E. (Ed.), *Progress in Optics*, Vol. XII, (North-Holland, Amsterdam).
- Slusher, R. E., S. Spalter, B. J. Eggleton, S. Pereira and J. E. Sipe, 2000, Bragg-grating-enhanced polarization instabilities, *Opt. Lett.* **25** (10), 749–751.
- Stegeman, G. I., and M. Segev, 1999, Optical spatial solitons and their interactions: Universality and diversity, *SCIENCE* **286** (5444), 1518–1523.
- Watanabe, K., H. Nakano, A. Honold and Y. Yamamoto, 1989, Optical nonlinearities of excitonic self-induced-transparency solitons: Toward ultimate realiza-

- tion of squeezed states and quantum nondemolition measurement, *Phys.Rev.Lett.* **62**, 2257.
- Winful, H. G., J. H. Marburger and E. Garmire, 1979, Theory of bistability in nonlinear distributed feedback structures, *Appl. Phys. Lett.* **35**, 379.
- Winful, H. G., and V. Perlin, 2000, Raman gap solitons, *Phys. Rev. Lett.* **84** (16), 3586 – 3589.
- Wright, E. M., 1991, Quantum theory of soliton propagation in an optical fiber using the Hartree approximation, *Phys.Rev.A* **43**, 3836 – 3844.
- Yablonovitch, E., 1987, Inhibited spontaneous emission in solid-state physics and electronics, *Phys. Rev. Lett.* **58** (20), 2059–2062.
- Yablonovitch, E., 1993, Photonic band-gap structures, *J. Opt. Soc. Am B* **10** (2), 283.
- Yudson, V. I., 1985, Dynamics of integrable quantum systems, *Sov.Phys.JETP* **61**, 1043.